Brain Structure and Function (2019) 224:1097–1117
https://doi.org/10.1007/s00429-018-01820-6

ORIGINAL ARTICLE

Basal forebrain subcortical projections

Lindsay J. Agostinelli[1,2] · Joel C. Geerling[1,2] · Thomas E. Scammell[1]

Received: 13 June 2018 / Accepted: 16 December 2018 / Published online: 5 January 2019

Abstract

The basal forebrain (BF) contains at least three distinct populations of neurons (cholinergic, glutamatergic, and GABAergic) across its different regions (medial septum, diagonal band, magnocellular preoptic area, and substantia innominata). Much attention has focused on the BF's ascending projections to cortex, but less is known about descending projections to subcortical regions. Given the neurochemical and anatomical heterogeneity of the BF, we used conditional anterograde tracing to map the patterns of subcortical projections from multiple BF regions and neurochemical cell types using mice that express Cre recombinase only in cholinergic, glutamatergic, or GABAergic neurons. We confirmed that different BF regions innervate distinct subcortical targets, with more subcortical projections arising from neurons in the caudal and lateral BF (substantia innominata and magnocellular preoptic area). Additionally, glutamatergic and GABAergic BF neurons have distinct patterns of descending projections, while cholinergic descending projections are sparse. Considering the intensity of glutamatergic and GABAergic descending projections, the BF likely acts through subcortical targets to promote arousal, motivation, and other behaviors.

Keywords Mice · Anterograde · Tracing · Substantia innominata · GABA · Acetylcholine

Abbreviations

3V	Third ventricle
AAV	Adeno-associated viral vector
ac	Anterior commissure
BF	Basal forebrain
BLA	Basolateral amygdala
BST (al)	Bed nucleus of the stria terminalis, anterolateral area
CEL	Central amygdala nucleus, lateral
CEM	Central amygdala nucleus, medial
ChAT	Choline acetyltransferase
ChR2	Channelrhodopsin-2
CM	Central medial nucleus of the thalamus
CPu	Caudate putamen
DAB	Diaminobenzidine
DMH	Dorsomedial hypothalamic nucleus
DR	Dorsal raphe
DTg	Dorsal tegmental nucleus
f	Fornix
GP	Globus pallidus
HDB	Horizontal nucleus of the diagonal band
IAM	Interanteromedial nucleus of the thalamus
ic	Internal capsule
IMD	Intermediodorsal nucleus of the thalamus
ip	Intraperitoneal
IPACm	Interstitial nucleus of the posterior limb of the anterior commissure, medial
IPN	Interpeduncular nucleus
LC	Locus coeruleus
LDT	Laterodorsal tegmental nucleus
LHb	Lateral habenula
LPB	Lateral parabrachial nucleus
LH	Lateral hypothalamus
LSD	Lateral septum, dorsal
LSI	Lateral septum, intermediate
LPO	Lateral preoptic area
MEA	Medial amygdala nucleus
MCPO	Magnocellular preoptic nucleus
MD	Mediodorsal nucleus of the thalamus
MHb	Medial habenula
MM	Medial mammillary nucleus

✉ Thomas E. Scammell
tscammel@bidmc.harvard.edu

[1] Department of Neurology, Beth Israel Deaconess Medical Center and Harvard Medical School, Boston, MA 02215, USA

[2] Department of Neurology, Roy J. and Lucille A. Carver College of Medicine, University of Iowa, Iowa City, IA 52242, USA

MPA	Medial preoptic area
MPB	Medial parabrachial nucleus
MPO	Medial preoptic nucleus
MRF	Medullary reticular formation
MS	Medial septum
NI	Nucleus incertus
NTS	Nucleus of the solitary tract
opt	Optic tract
PBel	Parabrachial nucleus, external lateral subnucleus
PCRt	Parvicellular reticular nucleus
PeF	Perifornical nucleus of the hypothalamus
PF	Parafascicular nucleus
PH	Posterior lateral hypothalamus
PPT	Pedunculopontine nucleus
PVH	Paraventricular nucleus of the hypothalamus
PVT	Paraventricular nucleus of the thalamus
RRF	Retrorubral field
SCN	Suprachiasmatic nucleus
scp	Superior cerebellar peduncle
SI	Substantia innominata
SNc	Substantia nigra: compact part
SNr	Substantia nigra: reticular part
st	Stria terminalis
STIA	Bed nucleus of the stria terminalis, intraamygdaloid
SUM	Supramammillary nucleus
TRN	Reticular nucleus of the thalamus
VDB	Vertical nucleus of the diagonal band
VTA	Ventral tegmental area
vPAG	Ventral periaqueductal gray
vGAT	Vesicular GABA transporter
vGluT1	Vesicular glutamate transporter, type 1
vGluT2	Vesicular glutamate transporter, type 2
vGluT3	Vesicular glutamate transporter, type 3
VMH	Ventromedial nucleus of the hypothalamus
VP	Ventral pallidum

Background or introduction

The basal forebrain (BF) is critical for arousal, attention, reward processing, and many other aspects of cognition (Voytko et al. 1994; Wilkinson et al. 1997; Martinez et al. 2005; Fuller et al. 2011; Brown et al. 2012; Fischer et al. 2014; Anaclet et al. 2015). Cortically projecting cholinergic neurons are present throughout the BF, and much attention has been given to cholinergic projections to the cortex (Rye et al. 1984; Saper 1984; Jones 2004; Goard and Dan 2009; Pinto et al. 2013; Han et al. 2014; Irmak and de Lecea 2014; Shi et al. 2015; Gielow and Zaborszky 2017). However, much less is known about the projections of glutamatergic and GABAergic neurons that extend throughout the length of the BF, from the medial septum (MS), vertical and horizontal limbs of the diagonal band (VDB and HDB), and back to the magnocellular preoptic nucleus (MCPO) and substantia innominata (SI) (Zaborszky and Duque 2003; Hur and Zaborszky 2005; Gritti et al. 2006; Xu et al. 2015).

Most BF research has focused on ascending projections, but descending projections are substantial and are likely to influence a variety of behaviors. BF neurons are thought to promote arousal, attention, and memory via ascending projections to the cortex (Rye et al. 1984; Gritti et al. 1997; Buzsaki et al. 1988; Jones 2004; Adamantidis et al. 2010; Han et al. 2014; Shi et al. 2015), but neurons in the MCPO and SI also project to wake-promoting orexin (hypocretin) neurons in the lateral hypothalamus (LH) (Yoshida et al. 2006; Henny and Jones 2006a; Agostinelli et al. 2017) and many other subcortical targets (Herkenham and Nauta 1977; Swanson et al. 1984; Grove 1988a; Semba 2000; Do et al. 2016). Prior studies of descending BF projections are limited in that they did not define the neurochemical subtypes of BF neurons, did not provide detailed information about how subcortical projections vary across BF regions, or did not include detailed information on targeted nuclei. Here, we describe the patterns of subcortical projections from different BF regions, and within in each region, we compare the projection patterns of neurons that release acetylcholine, glutamate, or GABA.

Methods

Animals

To selectively map the projections of BF neurons, we used female Cre-expressing mice weighing 20–30 g, $n = 15$–20 of each strain. These Cre knock-in mice have similar designs, with an IRES-Cre cassette inserted just after the stop codon of the gene coding for choline acetyltransferase (*Chat*), vesicular glutamate transporter 2 (*Vglut2; Slc17a6*), or vesicular GABA transporter (*Vgat; Slc32a1*). These mice were produced and characterized in the Lowell lab (Rossi et al. 2011; Vong et al. 2011), and they are available at The Jackson Laboratory (strain numbers 028861, 028863, 028862). Vglut2 is the vesicular glutamate transporter expressed by glutamatergic neurons in the BF, and Vglut1 is not expressed in the BF (Harkany et al. 2003; Nickerson Poulin et al. 2006; Henny and Jones 2006b); (http://mouse.brain-map.org). Vgat transports GABA into synaptic vesicles, and ChAT synthesizes acetylcholine. Mice presented in the current study were also used in a prior experiment focused on BF projections to orexin/hypocretin neurons in the lateral hypothalamus (Agostinelli et al. 2017).

We housed these mice on a 12:12 light:dark cycle with lights on at 0700 at 22 °C ambient temperature with

ad libitum access to food and water. All protocols and care of the mice followed National Institute of Health guidelines and were approved by the Beth Israel Deaconess Medical Center Institutional Animal Care and Use Committee.

Conditional anterograde tracing

We used conditional anterograde tracing to map projections of the three major populations of BF neurons. We injected the BF of Cre-expressing mice with an adeno-associated viral vector (AAV8-EF1α-DIO-hChR2(H134R)-mCherry, 6×10^{12} pfu/ml, UNC Vector Core) coding for Cre-dependent channelrhodopsin (ChR2) tagged with the red fluorescent protein mCherry (AAV-ChR2-mCherry). In this AAV, the ChR2-mCherry sequence is inverted and surrounded by pairs of loxP and lox2722 sites, thus limiting ChR2-mCherry expression to cells that contain Cre recombinase. By injecting this AAV into mice that express Cre recombinase selectively in GABAergic (Vgat-Cre), glutamatergic (Vglut2-Cre), or cholinergic (ChAT-Cre) neurons, we restricted ChR2-mCherry expression to neurochemically specific populations of BF neurons.

For stereotaxic delivery of this AAV, we first anesthetized mice with ketamine/xylazine (100/10 mg/kg. i.p.) and unilaterally microinjected 3–6 nl of AAV-ChR2-mCherry into the left BF. Injections were targeted at the major nuclei of the BF: medial septum (MS; AP + 0.74, RL 0.09, DV − 3.7 from the top of the skull); rostral part of the horizontal limb of the diagonal band of Broca (HDB; AP + 1.0, RL 0.45, DV − 5.1); caudal part of the horizontal limb of the diagonal band of Broca (HDB; AP + 0.4, RL 1.1, DV − 5.3); magnocellular preoptic nucleus (MCPO; + 0.4, RL 1.25, DV − 5.25); and substantia innominata (SI; AP − 0.12, RL 1.80, DV − 4.8) (Fig. 1).

Investigators debate the definition of the SI as it is anatomically complex and lacks clear boundaries (Canteras et al. 1995; Heimer et al. 1997; Alheid 2003; Agostinelli et al. 2017); just how the SI overlaps with the nucleus basalis, the ventral pallidum (VP), extended amygdala, and other structures in this region awaits the identification of more specific markers. We operationally define the SI as the loosely packed, subcommissural neurons within the field of magnocellular ChAT neurons dorsal to the more densely packed MCPO and HDB. Rostro-caudally, our SI injections ranged from just caudal to the decussation of the anterior commissure back to the caudal edge of the posterior limb of the anterior commissure.

An additional challenge is the heterogenous nature of the caudal BF, especially the SI. In addition to typical BF neurons, this region contains intermingled neurons of the extended amygdala and ventral pallidum, and teasing apart these populations is currently a challenge. We identify our SI injection sites relative to the VP which is usually defined by the wooly fiber projection from the ventral striatum (Heimer and Wilson 1975). Wooly fibers were initially identified in the VP by immunostaining for substance P and enkephalin (Haber and Nauta 1983), and we immunostained our injection sites for dynorphin which is expressed in ventral striatal neurons and axons that contain substance P (Fallon and Leslie 1986). Most of our SI injections lay caudal to the VP region containing dense dynorphin fiber labeling as there were no mCherry soma present on this level (Fig. 2). Caudally, at the level of our injection sites, the sparse dynorphin labeling was dorsal to the injection site. A few of the SI injection sites extended slightly into the ventral and caudal edge of the VP.

Four weeks after stereotaxic injection, we deeply anesthetized mice with ketamine/xylazine (150/15 mg/kg i.p.) and transcardially perfused them with 50 ml phosphate-buffered saline (PBS; pH 7.4) followed by 50 ml of buffered 10% formalin (pH 7.0; Fisher Scientific, Fair Lawn, NJ). We removed and postfixed the brains for 12 h in 10% formalin and then cryoprotected them in PBS containing 20% sucrose. We later sectioned the brains at 30 µm into a 1:4 series of coronal tissue sections on a freezing microtome.

Immunohistochemistry

We defined the BF by the boundaries of the cholinergic population as others have done previously (Hedreen et al. 1984; Schwaber et al. 1987; Semba 2000). To establish that our injections were within the borders of the BF, we double immunolabeled one series of sections from each mouse brown for ChAT with 3,3′-diaminobenzidine (DAB) and black for DsRed (which labels mCherry) with Ni-DAB (Fig. 1). Our immunostaining protocol followed the basic protocol described in Yoshida et al. (2006). In brief, we placed sections in 0.3% hydrogen peroxide prepared in PBT (PBS with 0.25% Triton X-100) for 30 min to inactivate endogenous peroxidases and then incubated them overnight in rabbit anti-DsRed (1:5,000; Clontech 632496, rabbit, polyclonal) and goat anti-ChAT (1:2,000; Millipore AB144P, goat, polyclonal) prepared in PBT with 3% normal horse serum. The next day, we incubated sections for 1 h in biotinylated donkey anti-rabbit IgG secondary antiserum (1:500; Jackson ImmunoResearch 711-065-152) followed by 1 h in avidin–biotin complex (Vectastain ABC Elite Kit; Vector Laboratories, Burlingame, CA). We labeled mCherry black with DAB in tris-buffered saline (TBS) with 0.024% hydrogen peroxide solution and 0.2% ammonium nickel (II) sulfate (Sigma). To visualize ChAT, we placed sections for 1 h in biotinylated donkey anti-goat IgG secondary antiserum (1:500; Jackson #705-065-147) followed by 1 h in ABC, and stained brown with DAB in TBS with 0.024% hydrogen peroxide.

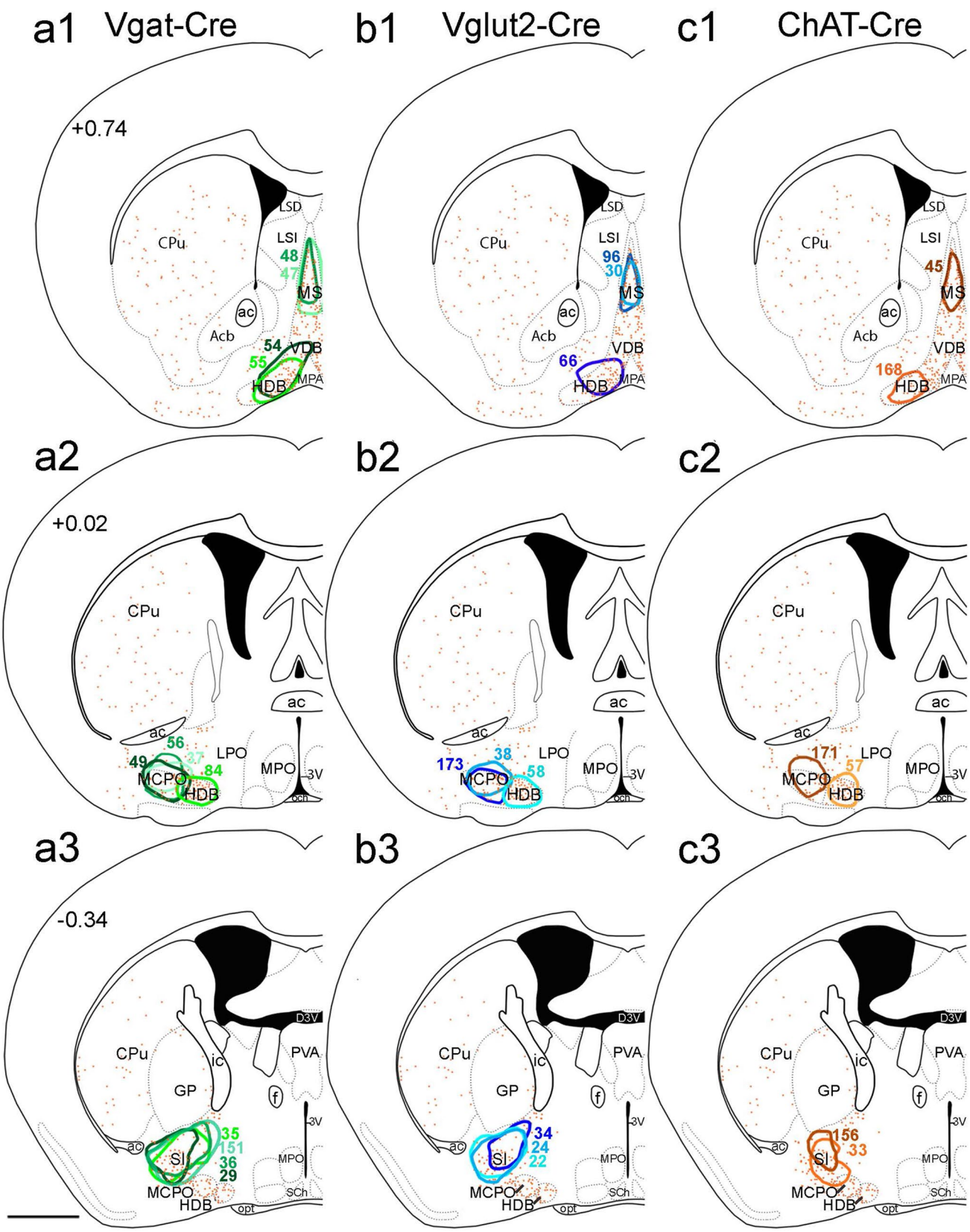

Fig. 1 Distribution of BF injection sites. (**a**1–**a**3) BF injection sites from Vgat-Cre mice, (**b**1–**b**3) Vglut-Cre mice, and (**c**1–**c**3) ChAT-Cre mice. Colored outlines show the boundary of each injection site. Orange dots show the distribution of cholinergic neurons, and atlas levels are per Franklin and Paxinos 2007. Scale bar 1 mm in A3 (applies to all panels)

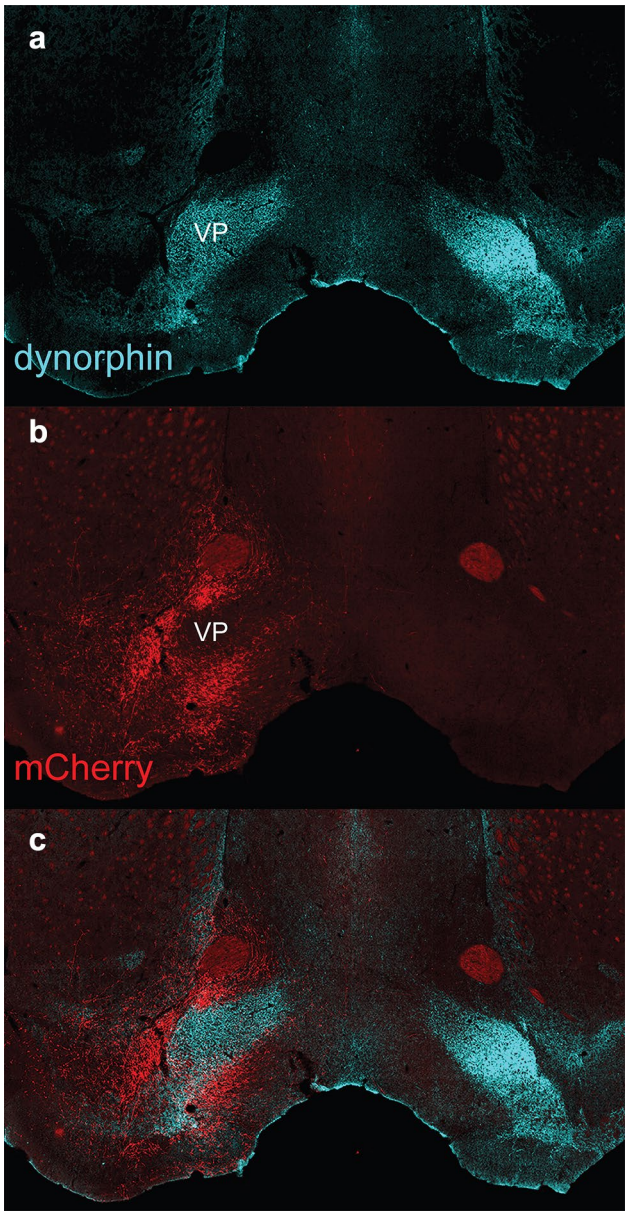

Fig. 2 GABAergic SI fibers (from case 35) labeled with mCherry (red) are distinct from and avoid the ventral pallidum (VP) as marked by the striatal dynorphinergic wooly fiber projection (blue)

To identify specific subcortical neurons, we labeled sections from some cases for additional markers. For example, after staining mCherry black with DAB, we incubated tissue overnight in donkey anti-orexin A (Santa Cruz Biotechnology, Cat# sc-8070, RRID AB_653610, goat, polyclonal) and proceeded to stain the orexin brown as described above. To examine the anatomic relationship between BF axons-specific brainstem neurons, we used double immunofluorescence labeling. After overnight incubation in rabbit anti-tyrosine hydroxylase (TH) (1:2,000; Millipore AB152), rat anti-mCherry (1:2,000; Life Technologies M11217), and goat anti-ChAT (1:1,000), we placed sections in donkey anti-rabbit IgG conjugated to Alexa Fluor 488 (1:500; Invitrogen A21206), donkey anti-rat conjugated to Cy3 (1:500; Jackson ImmunoResearch 712-165-153), and biotinylated donkey anti-goat IgG for 1 h, followed by PBS washes and then Cy5-conjugated streptavidin (1:1,000; Invitrogen; SA1001) for 1 h. Last, to map the VP, we stained forebrain sections for rabbit anti-dynorphin A (1:1,000; Peninsula T4268).

After immunolabeling, we mounted and dried sections on Superfrost Plus slides. For sections with fluorescence immunolabeling, we coverslipped with fade-retardant mounting medium containing DAPI (Vectashield; Vector Labs). For DAB-labeled tissue, we dehydrated sections in graded ethanols for 3 min each and cleared in xylenes for over an hour before coverslipping with a toluene-based mounting media (Cytoseal; Thermo Scientific).

After imaging the DAB-stained series with a slide scanner (Olympus VS120), we removed the coverslips and Nissl stained the sections in thionin for 30 s, followed by graded ethanol washes.

Validation of neurochemical specificity

Vgat- and Vglut2-Cre mice were previously characterized by crossing each to a Cre-reporter line (Vong et al. 2011) and comparing to gene expression in the Allen Brain Atlas (http://www.alleninstitute.org). To confirm that mCherry was expressed only in the correct types of neurons after AAV injections, we immunolabeled BF sections for mCherry and labeled cholinergic, glutamatergic, and GABAergic neurons by immunostaining for ChAT or using in situ hybridization to detect *Vgat* or *Vglut2* mRNA. In Chat-Cre mice, mCherry was expressed only in cholinergic neurons. In the Vglut2- and Vgat-Cre mice, 91% and 98% of the mCherry-labeled neurons contained *Vglut2* and *Vgat* mRNA, respectively (see Agostinelli et al. 2017). Additionally, in Vglut2- and Vgat-Cre mice, mCherry never co-localized with ChAT immunolabeling, confirming that BF Vgat and Vglut2 neurons are distinct from the cholinergic neurons (Gritti et al. 2006; Xu et al. 2015).

Analysis of anterograde tracing

We selected cases with mCherry-expressing neurons confined to the MS, HDB, MCPO, or SI ($n = 3$ for each region and for each Cre line). Cases were included if and only if mCherry + neurons were confined to the boundaries of the cholinergic BF neurons. We excluded 7/47 cases as misses (injections that hit the preoptic area, globus pallidus, and amygdala) and used them as anatomical controls to contrast with BF injections.

We plotted injection sites onto template drawings representing three levels of the BF (Fig. 1). Specifically, we

selected the central level of each injection site from 10X bright-field slide scanner images, then traced a border including all transduced cells from that central level onto a template using Photoshop (Adobe). In Fig. 1, the injection site boundaries encompass all labeled soma, but strongly labeled axons can make injection sites seem larger in some low magnification photos. For magnified view of the transfected soma inside cholinergic boundaries, please see Fig. 1 of Agostinelli et al. (2017).

To analyze subcortical BF projections, we used OlyVia software to view whole-slide images containing every section in the series. To quantify the density of axon terminals in subcortical structures, we used a qualitative scoring system of 0–3 with 0 = no axon terminals, 1 = a few axon terminals, 2 = moderate density of axon terminals, and 3 = heavy density of axon terminals.Table 1 lists all regions with BF axon terminals, plus a few relevant brain regions that lacked labeled terminals.

Results

Injection sites and general patterns of axonal labeling

We injected AAV-ChR2-mCherry into the BF of ChAT-Cre, Vglut2-Cre, and Vgat-Cre mice. The injection sites were relatively small, with rostro-caudal diameters of 720–960 µm (Fig. 1). We selected three cases limited to the MS, HDB, MCPO, or SI for each of the three lines of mice. Axons and terminals arising from the BF were strongly labeled with ChR2-mCherry in all cases. In general, glutamatergic and GABAergic neurons from a given BF region innervated many of the same regions, but there were several striking differences discussed below (Table 1). In contrast, the cholinergic neurons strongly innervated the cortex, including the hippocampus, but had sparse subcortical projections except to the basal amygdala and the reticular nucleus of the thalamus. Additionally, projections varied between BF regions, with more medial BF structures (MS and HDB) projecting to more medial subcortical regions and caudal-lateral BF structures projecting strongly to the lateral parts of the hypothalamus and brainstem.

Tracing from the rostral and caudal HDB produced very similar patterns of projections, so we grouped the cases together in Table 1. The MCPO projected to nearly identical targets as the SI, but with a lighter intensity (especially projections to the amygdala and medullary reticular formation in the GABAergic cases). Additionally, MCPO projected moderately to MS and HDB while SI had trace or light projections to these respective regions. In contrast, the MCPO glutamatergic projection to the mediodorsal (MD) thalamus and lateral habenula was as intense as that from the SI. For the sake of brevity, the MCPO is not listed in Table 1.

Cholinergic projections

Cholinergic neurons of the BF strongly innervated the cortex and hippocampus, but subcortical projections were limited. SI and MCPO cholinergic neurons projected heavily to the BLA (Fig. 3f), primarily targeting its anterior subdivision, and projected moderately to the medial subdivision of the central nucleus of the amygdala (CEM). HDB cholinergic axons targeted more caudal levels of the BLA, primarily the posterior subdivision. HDB cholinergic neurons moderately projected to the hippocampus and lightly projected to the reticular nucleus of the thalamus. MS cholinergic neurons moderately and exclusively innervated the hippocampus.

The cholinergic neurons of the HDB heavily projected to the MS, and this HDB to MS pathway was also clear in the GABAergic and glutamatergic cases. In contrast, cholinergic neurons of the SI and MS only sparsely innervated other BF regions (Table 1).

GABAergic projections

GABAergic BF neurons innervated many subcortical regions, and the pattern of projections varied across the rostral–caudal extent of the BF (Fig. 4).

Among all BF regions, GABAergic neurons of the SI and MCPO had the most extensive subcortical projections. GABAergic SI and MCPO neurons densely innervated an area referred to as the medial part of the interstitial nucleus of the posterior limb of the anterior commissure (IPACm) (Shammah-Lagnado et al. 2001), but avoided the ventral pallidum as defined by dynorphin wooly fiber labeling (Fig. 2). The mCherry + GABAergic neurons also strongly projected to the caudal nucleus accumbens core/BNST transition area and rostral–medial bed nucleus of the stria terminalis (BST), with labeling densest ventral and medial to the anterior commissure. GABAergic SI and MCPO fibers strongly innervated the olfactory tubercle, with dense terminals in the medial and superficial molecular layers. In the hypothalamus, GABAergic projections were densest in the LH, PH, and supramammillary nucleus (SUM), while completely sparing the medial mammillary nucleus (MM). The LH projection was densest over the level containing the orexin field (Fig. 3d), and tapered off more medially in the DMH and was absent in the VMH and SCN. SI and MCPO GABAergic neurons also densely innervated the CEM, ventral tegmental area (VTA), substantia nigra pars compacta (SNc), parasubthalamic nucleus, retrorubral field (RRF), and parabrachial nucleus. GABAergic SI projections even extended into the medulla, moderately innervating the pontine and medullary reticular formation (especially the parvicellular reticular

Table 1 Subcortical projection targets from three different BF cell types (GABA, glutamate, and acetylcholine) across three different BF structures (SI, HDB, MS)

	Substantia innominata			Horizontal nucl. of the diagonal band			Medial septum		
	Vglut2	Vgat	ChAT	Vglut2	Vgat	ChAT	Vglut2	Vgat	ChAT
BF									
MS	Trace	Trace	–	+++	+++	++	X	X	X
HDB	+	+	–	X	X	X	++	+++	Trace
MCPO	++	++	Trace	+	+	+	+	Trace	–
SI	X	X	X	–	–	Trace	–	–	–
Thalamus									
Anterodorsal	–	–	–	–	–	–	–	–	–
Anteroventral	–	–	–	–	+	–	–	–	–
Paratenial	+	+	–	+	+++	–	+	–	–
IMD	++	++	–	–	–	–	–	–	–
Mediodorsal	++	++	–	–	–	–	–	–	–
CM/ IAM	+	+	–	–	–	–	–	–	–
Reunions/rhomboid	++	+	–	–	–	–	+	–	–
Reticular (TRN)	–	+/++	–	–	+	+	–	–	–
PVT	+	+	–	–	–	–	–	–	–
PF (medial)	+	+	–	–	–	–	–	–	–
SubPF/PAG (rostral)	++	++	–	–	–	–	–	–	–
LHb (lateral)	+++	Trace	–	++	++	–	–	–	–
MHb	–	–	–	–	+++	–	–	+	–
Other forebrain regions									
Nucl. accumbens	+	++	–	–	–	–	–	–	–
Olfactory tubercle	+	++	–	–	–	–	–	–	–
CPu/GP	–	–	–	–	–	–	–	–	–
Hippocampus									
CA1-3	–	Trace	+	–	+	++	Trace	+++	++
Dentate gyrus	–	–	Trace	–	+	++	–	+++	Trace
Dorsal subiculum	–	–	–	–	++/+++	++	–	–	–
Ventral subiculum	–	+	–	–	+++	Trace	–	+	++
Amygdala and septum									
Triangular nu of septum	–	–	–	–	+++	+	Trace	+	–
Septofimbrial	–	–	–	–	+++	Trace	Trace	+	–
LSD	–	–	–	+++	–	–	–	–	–
LSI	+	–	–		–	–	Trace	–	–
BLA	–	Trace	+++	–	–	++	–	–	–
Lateral amygdala	–	–	–	–	–	–	–	–	–
Basomedial	+	++	+	–	–	+	–	–	–
CEM	++	+++	++	–	–	+/trace	–	–	–
CEL	–	–	–	–	–	–	–	––	–
MEA	+	+	–	–	+	–	–	–	–
Intercalated amygdala	++	++	–	–	–	–	–	–	–
STIA	++	++	–	–	–	–	–	–	–
BST (al)	++	++	–	–	+	–	–	–	–
Hypothalamus									
MPO	+	–	–	–	–	–	–	–	–
LPO	+	+	–	+	+	–	–	–	–
PVH	–	+	–	–	–	–	–	–	–
SCN	–	–	–	–	–	–	–	–	–
LH	++	++	–	+	+	–	+	+	–
DMH	+	+	–	–	–	–	–	–	–

Table 1 (continued)

	Substantia innominata			Horizontal nucl. of the diagonal band			Medial septum		
	Vglut2	Vgat	ChAT	Vglut2	Vgat	ChAT	Vglut2	Vgat	ChAT
PH	+	+++	–	–	+	–	Trace	+	–
SUM	++	+++	–	–	++	Trace	++	+	–
Mam (MM)	–	–	–	–	+++	–	–	Trace	–
Subthalamic	–	–	–	–	–	–	–	–	–
Parasubthalamic	+++	+++	–		–	–	–	–	–
Zona incerta	++	++	–	–	–	–	–	–	–
Brainstem									
SNc	++	+++	–	–	–	–	–	–	–
SNr	–	–	–	–	–	–	–	–	–
VTA	+++	+++	–	–	–	–	–	–	–
IPN	–	–	–	–	++	–	–	+	–
Red nucleus	–	–	–	–	–	–	–	–	–
RRF (A8)	++	+++	–	–	–	–	–	–	–
vPAG	++	++	–	–	–	–	–	–	–
PPT	+	+	–	–	–	–	–	–	–
Medial PB	+	++	–	–	–	–	–	–	–
Lateral PB	Trace	+++	–	–	–	–	–	–	–
LDT	+	Trace	–	–	–	–	–	Trace	–
Dorsal raphe (rostral)	++	++	–	+	+++	–	+	++	–
Dorsal raphe (caudal)	++	Trace	–	+	+++	–	+	++	–
Median raphe	++	Trace	–	+	++	–	+	+	–
Dorsal tegmental nucl.	–	–	–	–	–	–	–	–	–
LC	Trace	+	–	–	–	–	–	–	–
Pontine central gray	–	–	–	–	++	–	–	+	–
Nucleus incertus	+	–	–	Trace	+++	–	+	++	–
Subcoeruleus	Trace	++	–	–	–	–	–	–	–
Pontine reticular form.	+	+	–	–	–	–	–	–	–
Medullary reticular form.	–	++	–	–	–	–	–	–	–
NTS	–	++	–	–	–	–	–	–	–
Raphe magnus	+	+	–	–	–	–	–	–	–
Raphe obscurus	Trace	Trace	–	–	–	–	–	–	–

nucleus) and nucleus of the solitary tract. The SI and MCPO did not innervate the nucleus incertus (NI).

To examine these GABAergic projections in more detail, we triple labeled sections for TH, ChAT and mCherry. SI GABAergic fibers densely innervated many catecholaminergic brainstem regions, including the RRF (A8), SNc (A9), VTA (A10) (Fig. 5), and ventral PAG (A10dc, not shown). Axon terminals were sparse in the LC (A6) and the cholinergic PPT and LDT (Fig. 5e, c). In the parabrachial nucleus, the external lateral subnucleus (PBel) was densely innervated by GABAergic axons from the SI (Fig. 3j). Within PBel, these GABAergic fibers avoided the outer subdivision (Herbert et al. 1990) which contains TH-IR fibers (Fig. 5d), and instead concentrated in the inner PBel subdivision, which contained a few, small ChAT+ neurons. These GABAergic axons also densely innervated the PB medial and dorsal medial subnuclei surrounding the head of the superior cerebellar peduncle (scp) and extended caudally through the "waist area" (Fig. 5e). Additionally, at this level (and caudally where the nucleus is denser), the TH-labeled locus coeruleus had very sparse innervation from GABAergic SI neurons. However, GABAergic input from the SI was densest in the rostral portion of the laterodorsal tegmental nucleus (LDT).

GABAergic projections arising from the HDB often innervated different target regions than GABAergic neurons of the MCPO and SI. One of the densest HDB projections targeted the medial mammillary nucleus (MM), and this projection was similarly dense from the rostral (case 55) and caudal (case 84) HDB. In general, the HDB projected to regions near the midline including the triangular nucleus of the septum, septofimbrial nucleus, medial

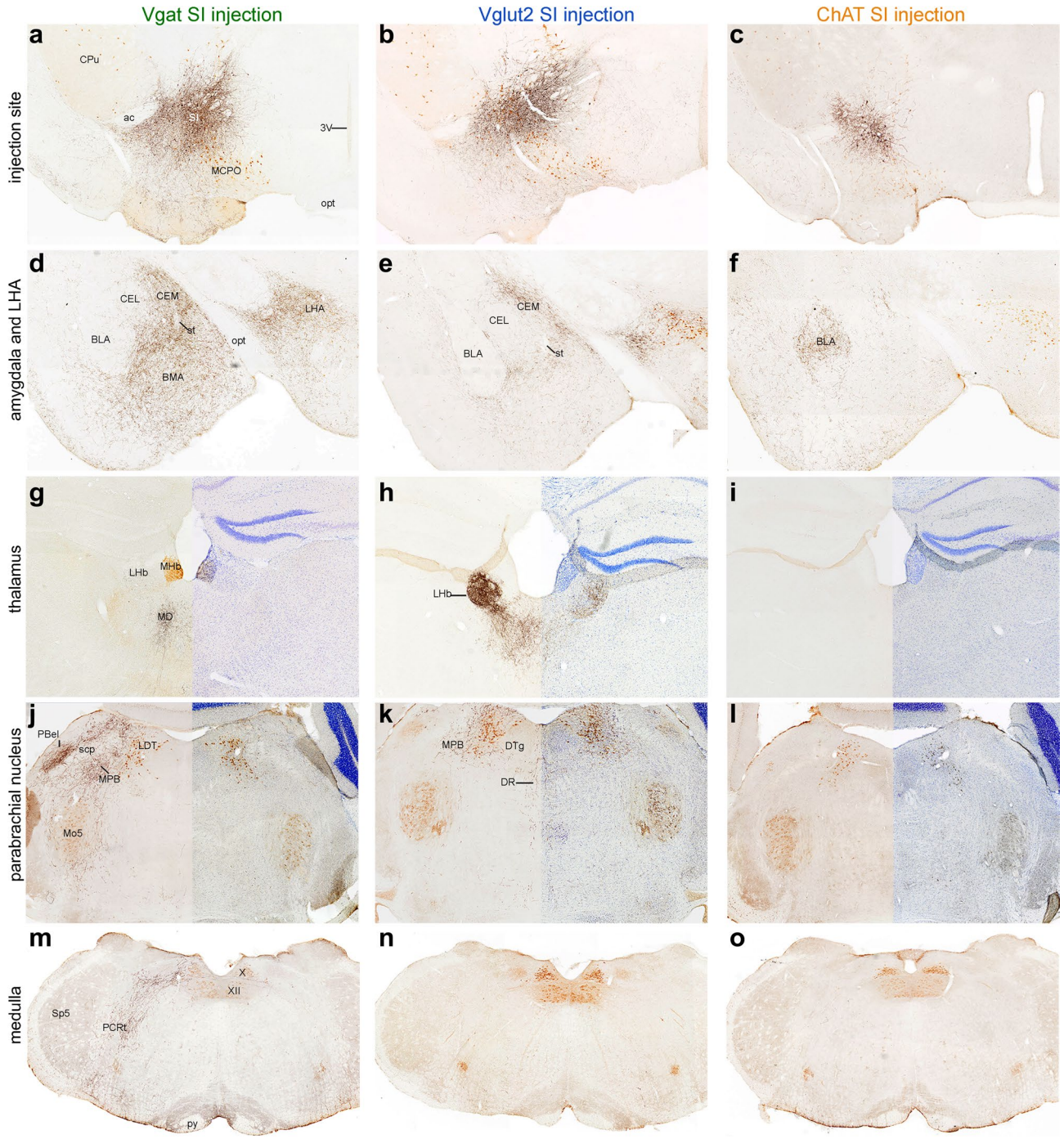

Fig. 3 Projections from different substantia innominata cell types. **a–c** Injection sites in the SI of Vgat (case 35), Vglut2 (case 34), and ChAT-Cre (case 156) mice. **d–o** Glutamatergic and GABAergic SI neurons vary in their projections to subcortical targets such as the amygdala, habenula, parabrachial nucleus, medullary reticular formation and NTS while cholinergic subcortical innervation is sparse outside of the BLA. mCherry fibers are labeled black with DAB+ Ni, orexin neurons are labeled in brown with DAB in the LH sections **d–f**, cholinergic cells are labeled brown with DAB in all other sections, and Nissl stain labels all cells in blue on the right side of **g–l**

habenula, MM, and interpeduncular nucleus. Additionally, compared to other BF regions, the GABAergic HDB fibers showed the densest projection to the dorsal raphe nucleus and the pontine central gray ventral to the dorsal tegmental nucleus (DTg) while completely avoiding the DTg (Fig. 4n). Just caudal to the dorsal raphe, the nucleus incertus was also heavily innervated by GABAergic HDB fibers, which extended across its full medial–lateral extent.

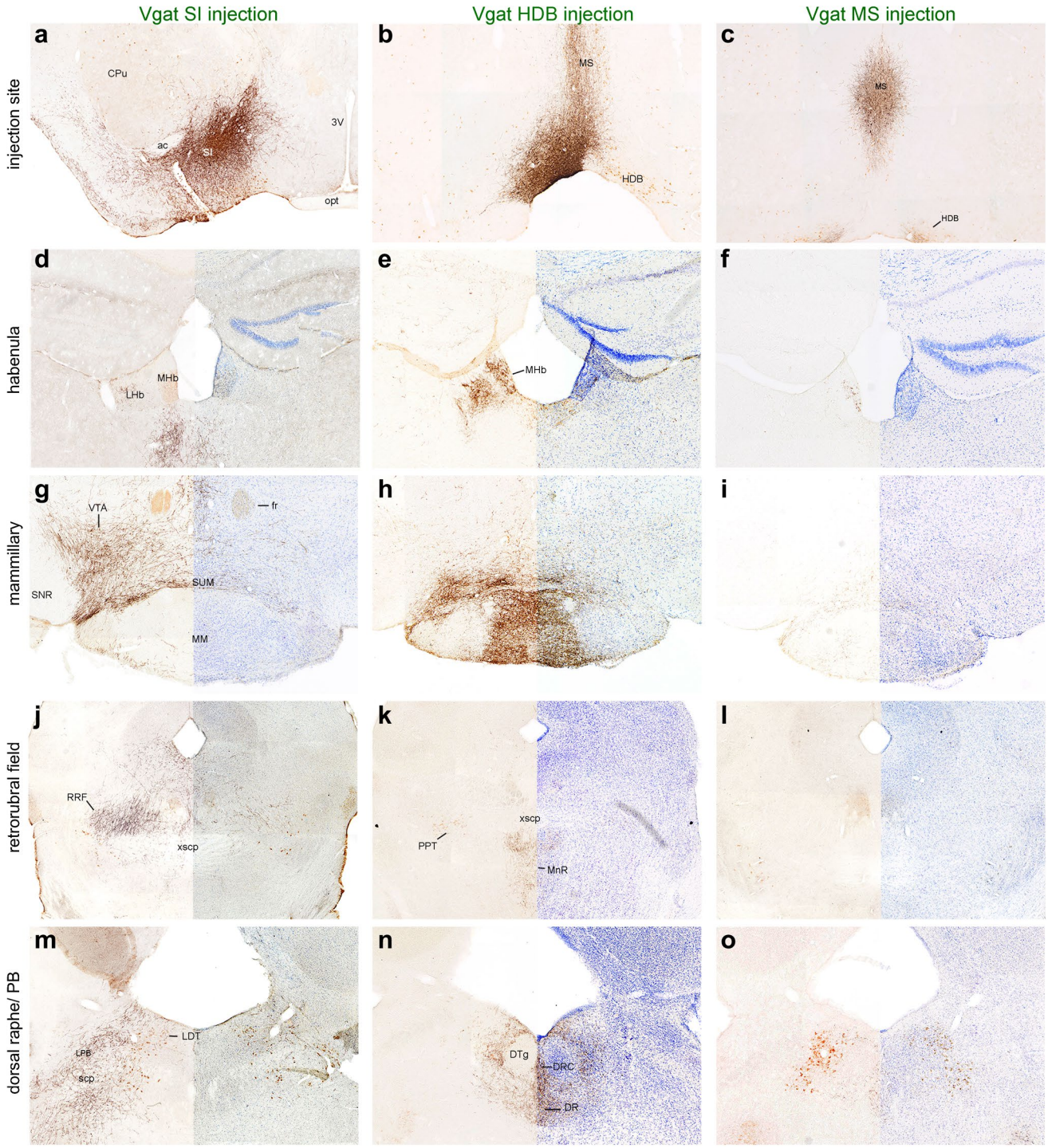

Fig. 4 GABAergic projections from different BF regions. **a**–**c** Injection sites in the SI (case 151), HDB (case 55), and MS (case 48) of vGAT-Cre mice. **d**–**o** GABAergic neurons from different BF regions show variation in projections to subcortical targets including the habenula, mammillary nuclei, RRF, PB, and DR. mCherry fibers are labeled black with DAB+ Ni, cholinergic cells are labeled brown with DAB, and Nissl stain in blue. The Nissl images are from the contralateral side of the brain

GABAergic neurons of the MS showed a pattern of descending projections similar to the HDB, but projections were generally lighter. These MS neurons heavily innervated the HDB and hippocampus, and lightly innervated the LH, PH, SUM, IPN and dorsal raphe. Like the HDB, these cells also moderately innervated the nucleus incertus.

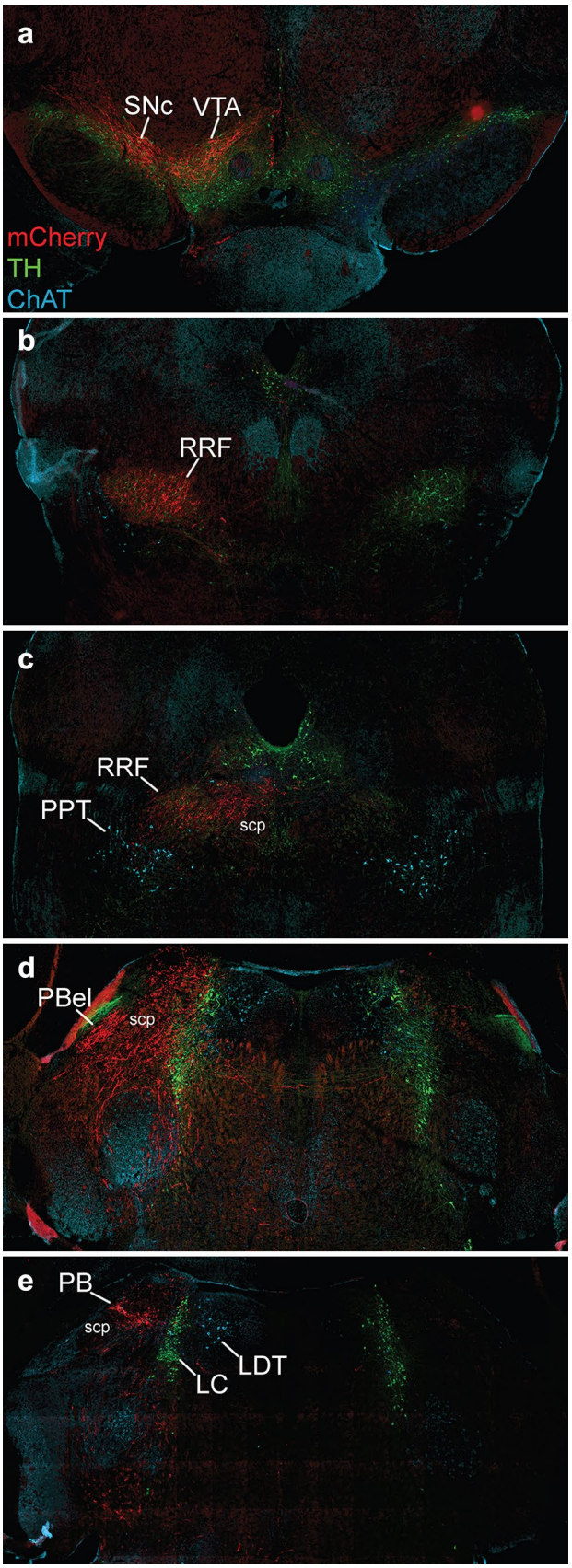

Fig. 5 SI inputs to brainstem catecholamine groups. mCherry-labeled ▶ GABAergic SI (case 151) neurons (red) sparsely project to ChAT neurons (blue) of the PPT and LDT while heavily projecting to TH-labeled neurons (green) in the VTA, SNc, and RRF (A8). mCherry fibers innervate the lateral PB, the PB "waist area" and caudal PBm, but avoid the outer portion of the PBel that is dense with tyrosine hydroxylase fibers, plus the LC and LDT

BF glutamatergic projections

BF glutamatergic neurons projected to many of the same subcortical regions as BF GABAergic neurons though there were some striking differences. Similar to the GABAergic neurons, the glutamatergic SI neurons innervated the BST, CEM (Fig. 3e), LH (especially the orexin field, Fig. 3e), SUM, VTA, RRF, medial parabrachial nucleus, and raphe magnus, while also avoiding the VMH, MM, DTg. However, the glutamatergic SI neurons very densely innervated the lateral habenula which contrasts sharply with the GABAergic SI neurons that provided only sparse innervation (Fig. 3g, h). In the ventral striatum, the glutamatergic SI neurons had a lighter and more diffuse projection to the olfactory tubercle than the GABAergic SI neurons which densely innervated the molecular layer and medial portions.

In addition, glutamatergic SI projections targeted fewer hindbrain regions in a pattern distinct from GABAergic SI neurons. For example, in the pons–midbrain, glutamatergic axons targeted the pontine central gray, a tegmental region medial to the PB, surrounding the LC and cholinergic LDT (Fig. 3k). In addition, glutamatergic SI neurons densely innervated the entire length of the dorsal raphe (not shown), whereas the GABAergic SI neurons mainly innervated the rostral part of the DR anterior to the rostral LDT. SI glutamatergic axons were rare in the medulla.

Glutamatergic neurons in the rostral and medial BF (MS and HDB) formed fewer subcortical forebrain projections than GABAergic neurons of the same BF regions. For example, glutamatergic neurons of the HDB and MS did not innervate the medial mammillary nucleus, medial habenula, or reticular nucleus of the thalamus. However, MS and HDB glutamatergic neurons lightly projected to the dorsal and median raphe, yet innervation was lighter than GABAergic projections from the same regions. The strongest projection of the glutamatergic HDB neurons was to the dorsal-most part of the LS (LSD) (Fig. 6). This glutamatergic projection was especially dense from the caudal HDB (case 58), moderate from the rostral HDB (case 66), and lacking from other BF regions or cell types.

Projections to the hippocampus

Though it is not a subcortical region, we also examined BF projections to the hippocampus. The densest hippocampal

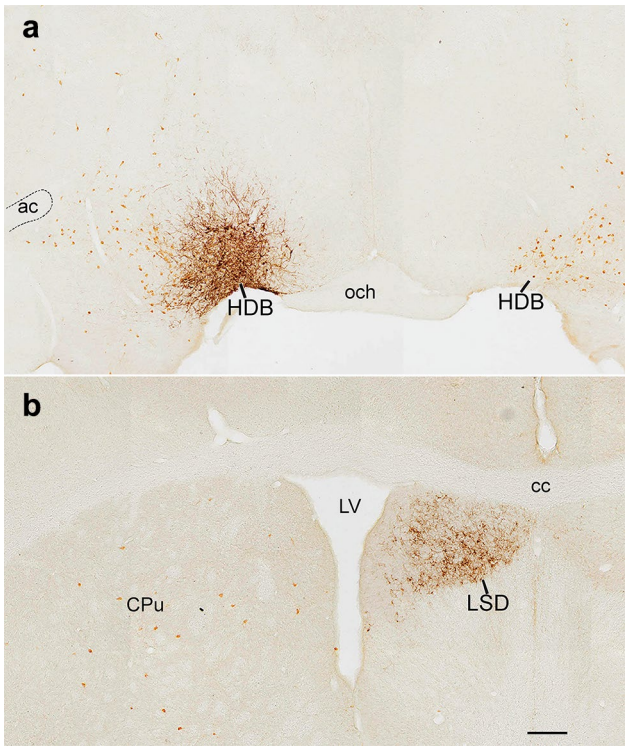

Fig. 6 Glutamatergic neurons of the HDB innervate the lateral septum. **a** Injection site in the caudal HDB (case 58) of a Vglut2-Cre mouse. mCherry labeled black with DAB+ Ni, cholinergic neurons are labeled brown with DAB. **b** mCherry labeled fibers (black) innervate the dorsal lateral septum (LSD). Scale bar is 200 um

projections came from GABAergic neurons in the MS, which heavily innervated caudal CA3 and ventral CA1 regions, the caudal polymorphic layer of the dentate gyrus, and less in the ventral subiculum but not the dorsal subiculum. HDB GABAergic axons lightly targeted similar hippocampal regions, but their projections to the dorsal and ventral subiculum were much denser. The MCPO and SI GABAergic neurons had sparse hippocampal projections limited to the ventral subiculum.

Similar to the GABAergic MS neurons, cholinergic neurons of the MS sent moderate projections to CA3 and CA1 neurons of the caudal hippocampus and ventral subiculum. In contrast, cholinergic axons from the HDB heavily projected to the rostral hippocampus (vs caudal hippocampus in MS cases) and dentate gyrus in the forebrain, then faded caudally, only projecting to the dorsal subiculum. Cholinergic projections from the SI were likely topographic; a more ventral injection (33) innervated the rostral hippocampus, but a more dorsal injection (156) labeled only a few axons in the hippocampus.

In contrast to the GABAergic and cholinergic neurons, glutamatergic BF neurons rarely projected to the hippocampus.

Control injections adjacent to the BF

We excluded seven cases as misses that hit areas adjacent to the BF (e.g., preoptic area, globus pallidus, and amygdala) and used them as anatomical controls to contrast with BF injections. Projections from the central amygdala in Vgat-Cre mice showed some similarities to those of the SI, as discussed in detail in the "Discussion" section, but these amygdala injections did not label projections to the cortex, reticular thalamus, or habenula as in the SI cases. Injections into the medial and lateral preoptic area labeled terminals in the caudal hypothalamus, but these avoided the portion of the LH medial to the fornix, and they had a sharp border outlining and avoiding the VMH that was not prominent in any of the BF cases. Preoptic injections into Vglut2-Cre and Vgat-Cre mice did not label projections to the lateral septum or medial mammillary nucleus, respectively, as described with HDB injections. In contrast to the SI injections, medial and lateral preoptic projections to the PB were sparse. Globus pallidus injections lacked most of the descending projections seen in the SI cases.

Discussion

Previous investigations of BF axonal projections have mainly used conventional tracers, and this study now defines the subcortical projections of GABAergic, glutamatergic, and cholinergic neurons from each BF region (summarized in Fig. 7). Much research on the BF has emphasized cortical projections, and studies of BF function often propose that behaviors are influenced via these cortical projections (Lin and Nicolelis 2008; Lin et al. 2015; Mayse et al. 2015). We and others have found that BF neurons have extensive subcortical projections that likely have important influences on behavior. Here, we place these new findings in the context of existing data and discuss the functional implications of this new information about the subcortical connectivity of the BF.

Comparison with previous literature

Grove used the anterograde axonal tracer *Phaseolus vulgaris* leucoagglutinin (PHA-L) and the retrograde tracer wheat germ agglutinin conjugated to horseradish peroxidase (WGA-HRP) to study the efferent projections of the SI in rats (Grove 1988a). Our findings in mice confirm much of the same general pattern, including projections to LH, VTA, SUM, and PB. However, we saw denser projections in the caudal brainstem (such as GABAergic SI projections to the NTS) than previously reported, probably due to stronger labeling of axons with highly expressed, cell membrane-targeted proteins such as ChR2 compared to conventional

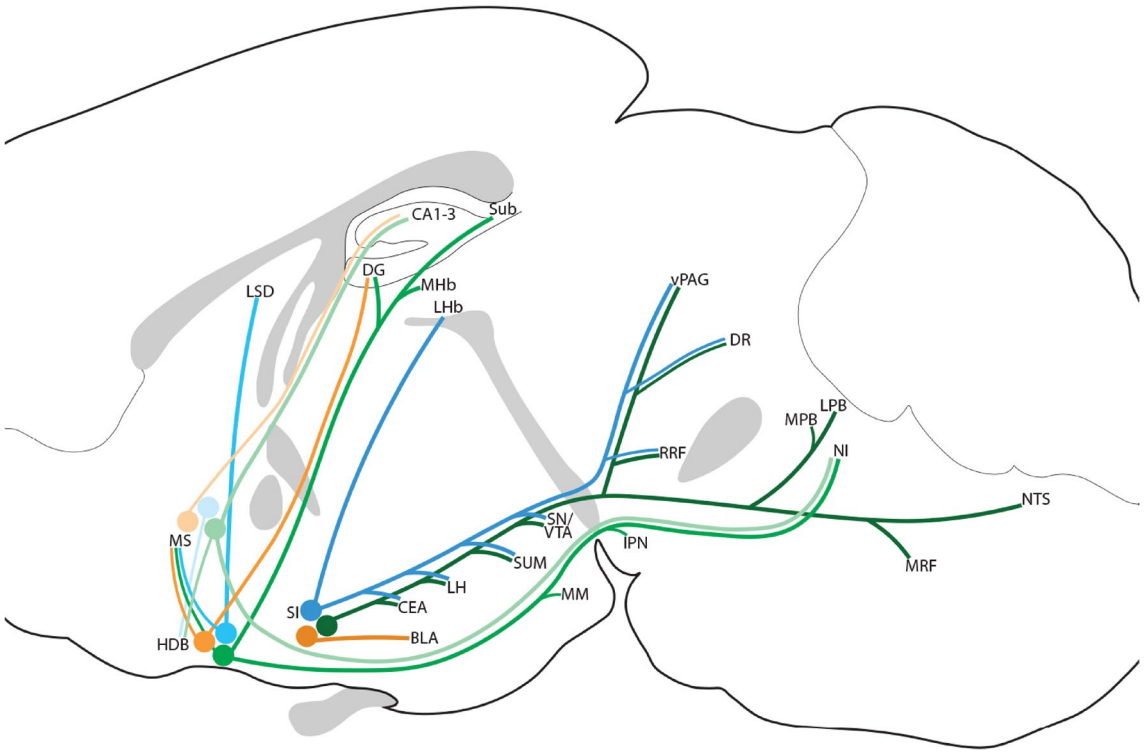

Fig. 7 Summary of subcortical projections of GABAergic (green), glutamatergic (blue), and cholinergic (orange) BF neurons from the MS, HDB, and SI

anterograde tracers. Our data also confirm Grove's conclusion that most descending projections of the SI originate from non-cholinergic neurons. Additionally, her paper suggests that neurons in the dorsal and ventral SI have some unique projections; our injections more closely resemble her dorsal SI pattern with projections to the pons and medulla. Last, similar to our data, Grove noted a striking difference in projections to the pons from the HDB (ventral to the SI), with HDB axons targeting more midline structures such as the dorsal and median raphe but not lateral structures such as the parabrachial nucleus. Based on our tracing data, it appears that most of this HDB projection arises from GABAergic neurons.

A more recent paper used a technique similar to ours for cell type-specific tracing of BF neurons, including the parvalbumin and somatostatin GABAergic subpopulations (Do et al. 2016). The injection sites in that study were much larger than ours (300–400 nl compared to our 3–6 nl AAV injections) and were meant to encompass the entire caudal portion of the BF (including HDB, MCPO, and SI). Most of their projection patterns appear similar to the sum of our projections across structures, but there were important differences: they reported a modest cholinergic projection to the hypothalamus that was absent in all our cases (they report using the same ChAT-Cre mice from Jackson Labs that we used here), and they did not identify the dense projections to pontine and medullary structures shown here. The stronger labeling of long-range axons in our study may be due to longer survival after AAV injection (4 weeks, compared to 2–3 weeks) and subsequently stronger, distal expression of ChR2-mCherry.

Lateral septum

Our anterograde tracing of glutamatergic HDB neurons revealed a strikingly dense projection to the dorsal-most part of the LS (LSD) (Fig. 6) that we did not see from other BF regions or cell types. This observation fits well with retrograde tracing from the dorsal LS in rats that revealed dense neuronal labeling in the HDB (Swanson and Cowan 1979).

The septal nuclei integrate and modify information from limbic cortical regions, primarily the hippocampus, and adjust motivated behaviors via output projections to the hypothalamus. Neurons in the region targeted by the HDB, the LSD, however, differ from other septal nuclei in that they only sparsely innervate the hippocampus and hypothalamus (Risold and Swanson 1997). PHA-L injection in the caudal dorsal LS (Fig. 22 of Risold and Swanson 1997) labeled a dense anterograde projection to the HDB, suggesting reciprocal connections between the dorsal LS and the glutamatergic HDB. At least some of this LSD projection targets cholinergic BF neurons that project to the medial prefrontal

cortex (Gielow and Zaborszky 2017), but this study did not discriminate between HDB and other BF regions. The nature of this LS-HDB circuit and its role relative to our conventional understanding of septal function remain unclear and require further investigation.

Thalamus

Kolmac and Mitrofanis used biotinylated dextrans to trace BF projections to the thalamus of rats, and our observations align with many of their conclusions (Kolmac and Mitrofanis 1999). For example, our tracing and their study show that several BF regions innervate the paratenial thalamus (PT), with the heaviest input arising from the HDB. Our tracing indicates that this HDB input to the PT is mainly GABAergic. Consistent with prior findings, we also see little to no innervation of principal relay nuclei other than MD. However, Kolmac and Mitrofanis reported that all BF structures innervate the MD nucleus, yet we found inputs only from the SI and MCPO but not from the HDB or MS.

Additionally, Kolmac and Mitrofanis report dense SI projections to the thalamic reticular nucleus (TRN) and sparse projections from VDB/HDB to only the ventral TRN in rats. We saw sparse yet more diffuse input to the TRN from the GABAergic SI and from the cholinergic and GABAergic HDB (in our mice, axons ascend further dorsally than in Kolmac and Mitrofanis Figure 2).

A few other studies examined the GABAergic projection from the BF to the TRN (Jourdain et al. 1989; Bickford et al. 1994). Activation of TRN cells drives neocortical spindle oscillations in NREM sleep (Halassa et al. 2011), and suppression of TRN activity increases accuracy in attentional visual tasks (Halassa et al. 2014). Perhaps, BF GABAergic neurons help inhibit the TRN during attentionally demanding tasks.

Habenula

Using nonspecific tracers, Herkenham and Nauta showed that the SI of rats innervates the lateral habenula (LHb) (see Fig. 3c, d), whereas the MS and HDB innervate the MHb (see Fig. 4a, b Herkenham and Nauta 1977). Our tracing shows a similar pattern, though we see very strong anterograde labeling from GABAergic HDB neurons (Fig. 4), and they showed surprisingly few retrogradely labeled cells in the HDB. A more recent study showed retrograde labeling of GABAergic neurons in the HDB and MS after tracer injection into the MHb of a GAD67-GFP reporter mouse (Qin and Luo 2009). Similarly, we found that the largest inputs to the MHb originated from GABAergic HDB neurons, whereas the densest projections to the LHb arise from glutamatergic SI and HDB neurons.

The MHb projects via the fasciculus retroflexus to the IPN, which, in part, modulates serotonergic raphe neurons implicated in sleep/wake and emotional regulation. The habenula is also implicated in suppressing motor activity, and destroying the fasciculus retroflexus decreases REM sleep and muscle atonia (Hikosaka 2010). Therefore, the BF GABAergic projection to the medial habenula might suppress REM sleep and enable motor activity that the MHb would otherwise suppress.

In contrast, the LHb projects to GABAergic neurons in the rostromedial tegmental nucleus (RTMg) which innervate and inhibit the dopaminergic VTA/SNc (Jhou et al. 2009, b; Hong et al. 2011). Via this pathway, electrical stimulation of the LHb inhibits midbrain dopaminergic neurons, while habenula lesions make animals hyperactive and distractible (Geisler and Trimble 2008; Hikosaka 2010). In addition, LHb neurons are activated when an animal receives a smaller than expected reward and inhibited by a large unexpected reward, which is the opposite pattern of dopaminergic neurons. (Matsumoto and Hikosaka 2007). Furthermore, LHb neurons are activated by stimuli indicating an aversive outcome (Matsumoto and Hikosaka 2007). The intense glutamatergic projection from the SI/MCPO to the LHb might provide this stimulus and increase dopaminergic inhibition to facilitate reward-based learning and decision-making, or suppress motor activity that may lead to aversive consequences.

Amygdala

The projection patterns of GABAergic neurons in several BF subregions are highly similar to those of GABAergic neurons in the central nucleus of the amygdala (discussed below), and they heavily innervate several regions of the amygdala. The SI gives rise to some of the densest amygdala projections, with a lighter projection from the MCPO, and there is a strong cholinergic projection from the SI and HDB. While GABAergic and glutamatergic SI neurons heavily innervate the CEM, the cholinergic neurons of the SI (and MCPO and HDB to a lesser extent) also project to the BLA. This cholinergic projection from the SI was first identified by retrograde tracing from the BLA (Carlsen et al. 1985; Woolf and Butcher 1982). As in the prior studies, we found most BLA-projecting neurons lie in the caudal, "sublenticular" part of the SI (see Figs. 3, 6e Carlsen et al. 1985).

The existence of a cholinergic BF projection to the cortical pyramidal neuron-like principal neurons in the BLA may simply parallel the broad, topographic projections from BF cholinergic neurons to the entire cerebral cortex (Price and Stern 1983; Saper 1984; Rye et al. 1984), yet the density of the projection to BLA is matched only by that to the hippocampus, suggesting an important role for cholinergic modulation in this region of the amygdala. A

previous study shows that BLA neurons densely express M1 muscarinic receptors (McDonald and Mascagni 2010), and these neurons exhibit excitatory or inhibitory responses to cholinergic input depending on cell type and basal activity level (Unal et al. 2015). For example, photostimulation of cholinergic BF fibers excites and activates BLA principal neurons and inhibits less active BLA neurons, and this pathway is thought to enhance the signal to noise response of BLA principal neurons to various stimuli.

Hypothalamus

BF neurons heavily target the caudal hypothalamus (LH, PH, SUM, and MM). In contrast, BF inputs to the preoptic and paraventricular nuclei were sparse, and we saw no innervation of the SCN.

In a previous study, we analyzed BF innervation of the orexin/hypocretin neurons in the LH (Agostinelli et al. 2017). We quantified the percentage of orexin neurons with GABAergic, glutamatergic, and cholinergic appositions from different BF regions and found a pattern similar to the qualitative data presented here: GABAergic and glutamatergic SI and MCPO neurons heavily projected to the orexin neurons, and cholinergic neurons did not. We also showed that SI glutamatergic axon terminals in the LH form functional, excitatory synapses on orexin neurons, and given that the orexin neurons are active during wake and help stabilize the waking state (Estabrooke et al. 2001; Mileykovskiy et al. 2005; Lee et al. 2005; Chemelli et al. 1999; Blouin et al. 2013), we hypothesized that this BF to orexin neuron projection may help maintain arousal.

In addition, the entire SUM is densely innervated by glutamatergic and GABAergic SI and GABAergic HDB neurons, with sparser projections from the glutamatergic and GABAergic MS neurons. Chemogenetic activation of glutamatergic SUM neurons produces long-lasting wakefulness, while inhibition decreases and fragments wake (Pedersen et al. 2017). In turn, SUM neurons project heavily to the hippocampus, throughout the dentate gyrus and CA2 (Wyss et al. 1979; Amaral and Cowan 1980; Haglund et al. 1984) and potently influence hippocampal theta rhythm (Kirk and McNaughton 1991; Kocsis and Vertes 1994; Vertes 2015). This pattern suggests that GABAergic and glutamatergic BF neurons may act via the SUM to influence arousal and hippocampal functions such as learning and spatial navigation.

We also found a heavy projection from GABAergic HDB neurons to the medial mammillary nucleus (MM). This HDB to MM projection was described previously in rats using conventional tracers (Shibata 1989; Gonzalo-Ruiz et al. 1992), and our new conditional tracing in mice suggests that this is a GABAergic projection. The mammillary bodies are a key link between hippocampal output and thalamocortical neurons in the classic circuit of Papez (1937). To the best of our knowledge, the GABAergic nature of this HDB to medial mammillary nucleus projection has not been described, yet it may also play a key role in memory.

A8/retrorubral field

GABAergic SI and MCPO neurons strongly projected to midbrain dopaminergic groups, including A8–A10. Zahm (2011) analyzed retrograde tracing from the medial to lateral span of the RRF, VTA, PAG, and SNc in rats and found dense retrograde labeling in the sublenticular extended amygdala (including the area that we refer to as the "SI") and CEL. Complementing our anterograde data, they did not see retrogradely labeled cells when they injected the SNr.

Dopamine neurons in these same midbrain regions project back to extended amygdala structures (Hasue and Shammah-Lagnado 2002; Yetnikoff et al. 2014), paralleling the well-known dopamine projections from SNc and VTA to the striatum. The GABAergic BF projections identified here may provide a direct negative feedback connection, which may dampen dopamine input to the central amygdala and related structures.

Pedunculopontine tegmental nucleus

Using PHA-L anterograde tracing in rats, Swanson and colleagues identified a projection from the SI to the midbrain, targeting a region they labeled the PPT (Swanson et al. 1984). Their midbrain and pontine projection pattern is broadly similar to what we observed in mice (see Fig. 4a–d Swanson et al. 1984), and their extracellular recordings in this region with SI stimulation revealed equal numbers of excitatory and inhibitory inputs around the PPT region, consistent with our finding that both GABAergic and glutamatergic SI neurons innervate this region.

However, we and others find that the SI mainly innervates the RRF rather than the PPT (Fig. 5). We initially thought that these glutamatergic and GABAergic BF projections to the midbrain tegmentum targeted the PPT as Swanson had claimed, but double labeling for ChAT and TH revealed that most SI axons do not enter the PPT but instead target A8, the catecholaminergic neurons in the RRF. In humans, the PPT borders are more expansive (Olszewski and Baxter 1953), but in rodents, the borders of the PPT are defined by the distribution of cholinergic (ChAT+) neurons (Armstrong et al. 1983; Rye et al. 1987), and in either case, the dopaminergic neurons of the RRF clearly lie rostral and dorsomedial to the PPT. Even at the level of the PPT, axons projecting from the BF were just dorsal to the PPT, heavily innervating the area marked by TH + fibers (Fig. 5c). Swanson's 1984 PHA-L study did not label for cholinergic or catecholaminergic neuron markers, but a few years later, Grove and colleagues also demonstrated that SI efferent fibers mainly course dorsal to

the cholinergic PPT soma (see Fig. 1h Grove 1988a, b). This pattern described by Grove is nearly identical to that seen in our glutamatergic and GABAergic SI and MCPO cases.

Parabrachial nucleus

GABAergic neurons in the SI and MCPO heavily project to several subregions of the PB. In the lateral PB, fibers innervate the inner portion of the external lateral subnucleus yet completely avoid the outer portion marked by TH-immunoreactive axons from the ventrolateral medulla and NTS (Milner et al. 1986). Additionally, we saw very dense projections to the "waist area" and medial PB. Our finding complements prior retrograde tracer injections in the PB that labeled many neurons in the SI (Moga et al. 1990; Tokita et al. 2009), and we now find that this BF input to the PB is GABAergic. The PB subnuclei targeted by the BF are largely the same regions that receive vagal and gustatory viscerosensory signals from the NTS (Herbert et al. 1990), suggesting that the GABAergic BF projections modulate taste and other visceral sensations.

The lateral PB is quite heterogeneous, and further studies are required to identify the PBel cell types that the GABAergic SI neurons innervate. The PBel contains several populations of cells, including cholinergic, CGRP+, glutamatergic, and other Lmx1b+ neurons. PBel neurons are activated by a wide variety of stimuli including sustained changes in blood pressure (Miller et al. 2012), visceral malaise (Carter et al. 2015; Campos et al. 2017), pain (Bernard et al. 1994; Campos et al. 2018), and hypercarbia (Yokota et al. 2015; Kaur et al. 2017). Activating PBel CGRP+ neurons awakens mice from sleep and produces anorexia and taste aversion (Carter et al. 2013, 2015). Conversely, inhibiting or ablating these CGRP+ neurons delays hypercapnia-induced arousals via the PB projection to the SI (Kaur et al. 2017), reduces freezing responses to foot shock pain (Han et al. 2015), and ameliorates the normal anorexic effects of toxins and cancer (Campos et al. 2017). The diversity of stimuli and functions has led to the suggestion that the CGRP neurons operate as a sort of "house alarm" for the brain (Saper 2016; Palmiter 2018). PBel CGRP+ neurons mediate their alerting and aversive effects in large part by output projections to the CeA and SI (Carter et al. 2013; Kaur et al. 2017; Campos et al. 2017), and we propose that these neurons may receive a negative feedback projection from the same regions.

Nucleus incertus

We found a major projection to the NI from GABAergic HDB neurons and a lighter projection from GABAergic MS neurons. Our findings complement a previous retrograde tracing study showing afferent projections to the NI in rat, primarily from the HDB (Goto et al. 2001), and we find that this BF input is largely GABAergic. Surprisingly, GABAergic SI neurons did not innervate the NI, even though they give rise to the heaviest brainstem projections overall. The NI projects back to the MS and HDB and helps drive hippocampal theta rhythm (Brown and McKenna 2015), and electrical stimulation of the NI can induce theta rhythm in the hippocampus (Nunez et al. 2006). It is possible that the reciprocal connections between HDB and NI contribute to theta rhythmogenesis.

Comparison of SI, amygdala, and BNST projections

The descending projections of GABAergic SI neurons are similar to those of GABAergic neurons in the CEA, especially its medial subdivision (CEM) and parts of the BNST. Alheid and Heimer proposed the idea of a "central extended amygdala", suggesting that these neurons might form a continuum, with amygdala-like neurons scattered through the SI (Alheid and Heimer 1988). Axonal tracing in multiple species has shown CEM projections to PAG, PB, catecholaminergic groups, and other brainstem structures, similar to the SI projections we describe here (Hopkins and Holstege 1978; Price and Amaral 1981; Veening et al. 1984; Moga et al. 1990; Rizvi et al. 1991; Wallace et al. 1992; Petrovich and Swanson 1997). Descending projections to these target regions from the vicinity of the CEA regulate a wide variety of effects including fear-induced freezing (Tovote et al. 2016), REM sleep (Lu et al. 2006), cataplexy (Burgess et al. 2013; Mahoney et al. 2017) and respiration (Dlouhy et al. 2015). Two studies in 1988 by Grove reveal the afferent and efferent connections of the SI, and her discussion considers the striking similarities between some SI, CEA and lateral BST projections (Grove 1988a, b). These regions share similar neurotransmitters and projection patterns (Cassell et al. 1986; Gray and Magnuson 1987) and can even show similar patterns of activity (Scammell et al. 1998; Elmquist et al. 1996; Ericsson et al. 1994). A major distinction is that the SI projects to the cortex, reticular nucleus of the thalamus, and lateral habenula, while the CEA does not. Further studies targeting specific populations over the length of the BST–SI–CEA continuum will be necessary to distinguish cell types and functions.

Limitations

To study glutamatergic projections, we focused on BF neurons containing Vglut2 as this transporter is expressed by the vast majority of glutamatergic BF neurons. Still, a few ChAT and potentially parvalbumin-containing BF neurons contain Vglut3 (Harkany et al. 2003; Nickerson Poulin et al. 2006; Gritti et al. 2006) and it is possible that some cholinergic BF neurons co-release glutamate, as has been

shown in cholinergic interneurons in the striatum (Higley et al. 2011). Whether the projection pattern of Vglut3 + BF cholinergic neurons differs from the projections of other cholinergic neurons is unclear, but it could be addressed using similar tracing methods in Vglut3-Cre mice.

As discussed previously, nomenclature pertaining to the SI, VP, MCPO, extended amygdala and other subregions varies between labs, in part because the SI/VP region is a complex intersection of BF, pallidal, striatal, and amygdala-related neurons. We operationally defined the SI by the bounds of the cholinergic neurons in line with prior BF research, but this region contains intermixed neuronal populations. Our conditional tracing was helpful in limiting mCherry expression to GABAergic neurons, but as Vgat is expressed in SI, VP, and extended amygdala neurons, our SI cases probably label axons from more than one type of neuron. An important goal of future research will be to identify more specific neuronal markers in and around the SI to disentangle these populations and their functions.

Conclusions

Most BF research has focused on ascending projections to the cortex, but our experiments highlight the large and numerous descending projections of the BF. Our identification of a large GABAergic projection from HDB to the mammillary bodies, along with the dense HDB projection to the output region of the hippocampus (subiculum), and other BF projections to the lateral habenula, lateral hypothalamus, SUM, and nucleus incertus should revise the way we view the output pathways through which the BF can influence learning, motivation, and memory. Many current models focus predominantly on projections of cholinergic BF neurons to the cerebral cortex, particularly those from the MS to the hippocampus, but our findings indicate that other BF neurons—primarily non-cholinergic and outside the MS—are positioned to exert heavy subcortical influence over negative valence learning signals via the habenula, and hippocampal memory consolidation via the MM, SUM, NI, and the subiculum. Selectively testing these non-cholinergic projections for their effects on learning and memory is now possible using Cre-dependent targeting similar to our conditional tracing approach. This information could hold important insights for Alzheimer's and other neurodegenerative diseases where basal forebrain neurodegeneration has been identified, but cholinergic drug therapy has had limited clinical impact.

Funding NIH P01 HL095491 to TS, NIH P01 HL095491-02S1 to LJA.

Compliance with ethical standards

Conflict of interest The authors declare that they have no conflict of interest.

Ethical approval All applicable international, national, and/or institutional guidelines for the care and use of animals were followed.

References

Adamantidis A, Carter MC, de Lecea L (2010) Optogenetic deconstruction of sleep-wake circuitry in the brain. Front Mol Neurosci 2:31. https://doi.org/10.3389/neuro.02.031.2009

Agostinelli LJ, Ferrari LL, Mahoney CE, Mochizuki T, Lowell BB, Arrigoni E, Scammell TE (2017) Descending projections from the basal forebrain to the orexin neurons in mice. J Comp Neurol 525(7):1668–1684. https://doi.org/10.1002/cne.24158

Alheid GF (2003) Extended amygdala and basal forebrain. Ann N Y Acad Sci 985:185–205

Alheid GF, Heimer L (1988) New perspectives in basal forebrain organization of special relevance for neuropsychiatric disorders: the striatopallidal, amygdaloid, and corticopetal components of substantia innominata. Neuroscience 27(1):1–39

Amaral DG, Cowan WM (1980) Subcortical afferents to the hippocampal formation in the monkey. J Comp Neurol 189(4):573–591. https://doi.org/10.1002/cne.901890402

Anaclet C, Pedersen NP, Ferrari LL, Venner A, Bass CE, Arrigoni E, Fuller PM (2015) Basal forebrain control of wakefulness and cortical rhythms. Nat Commun 6:8744. https://doi.org/10.1038/ncomms9744

Armstrong DM, Saper CB, Levey AI, Wainer BH, Terry RD (1983) Distribution of cholinergic neurons in rat brain: demonstrated by the immunocytochemical localization of choline acetyltransferase. J Comp Neurol 216(1):53–68. https://doi.org/10.1002/cne.902160106

Bernard JF, Huang GF, Besson JM (1994) The parabrachial area: electrophysiological evidence for an involvement in visceral nociceptive processes. J Neurophysiol 71(5):1646–1660. https://doi.org/10.1152/jn.1994.71.5.1646

Bickford ME, Gunluk AE, Van Horn SC, Sherman SM (1994) GABAergic projection from the basal forebrain to the visual sector of the thalamic reticular nucleus in the cat. J Comp Neurol 348(4):481–510. https://doi.org/10.1002/cne.903480402

Blouin AM, Fried I, Wilson CL, Staba RJ, Behnke EJ, Lam HA, Maidment NT, Karlsson KAE, Lapierre JL, Siegel JM (2013) Human hypocretin and melanin-concentrating hormone levels are linked to emotion and social interaction. Nat Commun 4:1547. https://doi.org/10.1038/ncomms2461

Brown RE, McKenna JT (2015) Turning a negative into a positive: ascending GABAergic control of cortical activation and arousal. Front Neurol 6:135. https://doi.org/10.3389/fneur.2015.00135

Brown RE, Basheer R, McKenna JT, Strecker RE, McCarley RW (2012) Control of sleep and wakefulness. Physiol Rev 92(3):1087–1187. https://doi.org/10.1152/physrev.00032.2011

Burgess CR, Oishi Y, Mochizuki T, Peever JH, Scammell TE (2013) Amygdala lesions reduce cataplexy in orexin knock-out mice. J Neurosci 33(23):9734–9742. https://doi.org/10.1523/JNEUROSCI.5632-12.2013

Buzsaki G, Bickford RG, Ponomareff G, Thal LJ, Mandel R, Gage FH (1988) Nucleus basalis and thalamic control of neocortical activity in the freely moving rat. J Neurosci 8(11):4007–4026

Campos CA, Bowen AJ, Han S, Wisse BE, Palmiter RD, Schwartz MW (2017) Cancer-induced anorexia and malaise are mediated

by CGRP neurons in the parabrachial nucleus. Nat Neurosci 20(7):934–942. https://doi.org/10.1038/nn.4574

Campos CA, Bowen AJ, Roman CW, Palmiter RD (2018) Encoding of danger by parabrachial CGRP neurons. Nature 555(7698):617–622. https://doi.org/10.1038/nature25511

Canteras NS, Simerly RB, Swanson LW (1995) Organization of projections from the medial nucleus of the amygdala: a PHAL study in the rat. J Comp Neurol 360(2):213–245. https://doi.org/10.1002/cne.903600203

Carlsen J, Zaborszky L, Heimer L (1985) Cholinergic projections from the basal forebrain to the basolateral amygdaloid complex: a combined retrograde fluorescent and immunohistochemical study. J Comp Neurol 234(2):155–167. https://doi.org/10.1002/cne.902340203

Carter ME, Soden ME, Zweifel LS, Palmiter RD (2013) Genetic identification of a neural circuit that suppresses appetite. Nature 503(7474):111–114. https://doi.org/10.1038/nature12596

Carter ME, Han S, Palmiter RD (2015) Parabrachial calcitonin gene-related peptide neurons mediate conditioned taste aversion. J Neurosci 35(11):4582–4586. https://doi.org/10.1523/JNEUROSCI.3729-14.2015

Cassell MD, Gray TS, Kiss JZ (1986) Neuronal architecture in the rat central nucleus of the amygdala: a cytological, hodological, and immunocytochemical study. J Comp Neurol 246(4):478–499. https://doi.org/10.1002/cne.902460406

Chemelli RM, Willie JT, Sinton CM, Elmquist JK, Scammell T, Lee C, Richardson JA, Williams SC, Xiong Y, Kisanuki Y, Fitch TE, Nakazato M, Hammer RE, Saper CB, Yanagisawa M (1999) Narcolepsy in orexin knockout mice: molecular genetics of sleep regulation. Cell 98(4):437–451

Dlouhy BJ, Gehlbach BK, Kreple CJ, Kawasaki H, Oya H, Buzza C, Granner MA, Welsh MJ, Howard MA, Wemmie JA, Richerson GB (2015) Breathing inhibited when seizures spread to the amygdala and upon amygdala stimulation. J Neurosci 35(28):10281–10289. https://doi.org/10.1523/JNEUROSCI.0888-15.2015

Do JP, Xu M, Lee SH, Chang WC, Zhang S, Chung S, Yung TJ, Fan JL, Miyamichi K, Luo L, Dan Y (2016) Cell type-specific long-range connections of basal forebrain circuit. Elife. https://doi.org/10.7554/eLife.13214

Elmquist JK, Scammell TE, Jacobson CD, Saper CB (1996) Distribution of Fos-like immunoreactivity in the rat brain following intravenous lipopolysaccharide administration. J Comp Neurol 371 (1):85–103. https://doi.org/10.1002/(SICI)1096-9861(19960715)371:1<85::AID-CNE5>3.0.CO;2-H

Ericsson A, Kovacs KJ, Sawchenko PE (1994) A functional anatomical analysis of central pathways subserving the effects of interleukin-1 on stress-related neuroendocrine neurons. J Neurosci 14(2):897–913

Estabrooke IV, McCarthy MT, Ko E, Chou TC, Chemelli RM, Yanagisawa M, Saper CB, Scammell TE (2001) Fos expression in orexin neurons varies with behavioral state. J Neurosci 21(5):1656–1662

Fallon JH, Leslie FM (1986) Distribution of dynorphin and enkephalin peptides in the rat brain. J Comp Neurol 249(3):293–336. https://doi.org/10.1002/cne.902490302

Fischer TH, Eiringhaus J, Dybkova N, Forster A, Herting J, Kleinwachter A, Ljubojevic S, Schmitto JD, Streckfuss-Bomeke K, Renner A, Gummert J, Hasenfuss G, Maier LS, Sossalla S (2014) Ca(2+) /calmodulin-dependent protein kinase II equally induces sarcoplasmic reticulum Ca(2+) leak in human ischaemic and dilated cardiomyopathy. Eur J Heart Fail 16(12):1292–1300. https://doi.org/10.1002/ejhf.163

Franklin KB, Paxinos G (2007) The mouse brain in stereotaxic coordinates. Elsevier, Amsterdam

Fuller PM, Sherman D, Pedersen NP, Saper CB, Lu J (2011) Reassessment of the structural basis of the ascending arousal system. J Comp Neurol 519(5):933–956. https://doi.org/10.1002/cne.22559

Geisler S, Trimble M (2008) The lateral habenula: no longer neglected. CNS Spectr 13(6):484–489

Gielow MR, Zaborszky L (2017) The Input–output relationship of the cholinergic basal forebrain. Cell Rep 18(7):1817–1830. https://doi.org/10.1016/j.celrep.2017.01.060

Goard M, Dan Y (2009) Basal forebrain activation enhances cortical coding of natural scenes. Nat Neurosci 12(11):1444–1449. https://doi.org/10.1038/nn.2402

Gonzalo-Ruiz A, Alonso A, Sanz JM, Llinas RR (1992) Afferent projections to the mammillary complex of the rat, with special reference to those from surrounding hypothalamic regions. J Comp Neurol 321(2):277–299. https://doi.org/10.1002/cne.903210208

Goto M, Swanson LW, Canteras NS (2001) Connections of the nucleus incertus. J Comp Neurol 438(1):86–122

Gray TS, Magnuson DJ (1987) Neuropeptide neuronal efferents from the bed nucleus of the stria terminalis and central amygdaloid nucleus to the dorsal vagal complex in the rat. J Comp Neurol 262(3):365–374. https://doi.org/10.1002/cne.902620304

Gritti I, Mainville L, Mancia M, Jones BE (1997) GABAergic and other noncholinergic basal forebrain neurons, together with cholinergic neurons, project to the mesocortex and isocortex in the rat. J Comp Neurol 383(2):163–177

Gritti I, Henny P, Galloni F, Mainville L, Mariotti M, Jones BE (2006) Stereological estimates of the basal forebrain cell population in the rat, including neurons containing choline acetyltransferase, glutamic acid decarboxylase or phosphate-activated glutaminase and colocalizing vesicular glutamate transporters. Neuroscience 143(4):1051–1064. https://doi.org/10.1016/j.neuroscience.2006.09.024

Grove EA (1988a) Efferent connections of the substantia innominata in the rat. J Comp Neurol 277(3):347–364

Grove EA (1988b) Neural associations of the substantia innominata in the rat: afferent connections. J Comp Neurol 277(3):315–346. https://doi.org/10.1002/cne.902770302

Haber SN, Nauta WJ (1983) Ramifications of the globus pallidus in the rat as indicated by patterns of immunohistochemistry. Neuroscience 9(2):245–260

Haglund L, Swanson LW, Kohler C (1984) The projection of the supramammillary nucleus to the hippocampal formation: an immunohistochemical and anterograde transport study with the lectin PHA-L in the rat. J Comp Neurol 229(2):171–185. https://doi.org/10.1002/cne.902290204

Halassa MM, Siegle JH, Ritt JT, Ting JT, Feng G, Moore CI (2011) Selective optical drive of thalamic reticular nucleus generates thalamic bursts and cortical spindles. Nat Neurosci 14(9):1118–1120. https://doi.org/10.1038/nn.2880

Halassa MM, Chen Z, Wimmer RD, Brunetti PM, Zhao S, Zikopoulos B, Wang F, Brown EN, Wilson MA (2014) State-dependent architecture of thalamic reticular subnetworks. Cell 158(4):808–821. https://doi.org/10.1016/j.cell.2014.06.025

Han Y, Shi YF, Xi W, Zhou R, Tan ZB, Wang H, Li XM, Chen Z, Feng G, Luo M, Huang ZL, Duan S, Yu YQ (2014) Selective activation of cholinergic basal forebrain neurons induces immediate sleep-wake transitions. Curr Biol 24(6):693–698. https://doi.org/10.1016/j.cub.2014.02.011

Han S, Soleiman MT, Soden ME, Zweifel LS, Palmiter RD (2015) Elucidating an affective pain circuit that creates a threat memory. Cell 162(2):363–374. https://doi.org/10.1016/j.cell.2015.05.057

Harkany T, Hartig W, Berghuis P, Dobszay MB, Zilberter Y, Edwards RH, Mackie K, Ernfors P (2003) Complementary distribution of type 1 cannabinoid receptors and vesicular glutamate transporter 3 in basal forebrain suggests input-specific retrograde signalling by cholinergic neurons. Eur J Neurosci 18(7):1979–1992

Hasue RH, Shammah-Lagnado SJ (2002) Origin of the dopaminergic innervation of the central extended amygdala and accumbens shell: a combined retrograde tracing and immunohistochemical study in the rat. J Comp Neurol 454(1):15–33. https://doi.org/10.1002/cne.10420

Hedreen JC, Struble RG, Whitehouse PJ, Price DL (1984) Topography of the magnocellular basal forebrain system in human brain. J Neuropathol Exp Neurol 43(1):1–21

Heimer L, Wilson RD (1975) The subcortical projections of the allocortex: similarities in the neural associations of the hippocampus, the piriform cortex, and the neocortex. In: M. Santini (ed) Golgi Centennial Symposium, Raven Press, New York, pp 177–193

Heimer L, Harlan RE, Alheid GF, Garcia MM, de Olmos J (1997) Substantia innominata: a notion which impedes clinical-anatomical correlations in neuropsychiatric disorders. Neuroscience 76(4):957–1006

Henny P, Jones BE (2006a) Innervation of orexin/hypocretin neurons by GABAergic, glutamatergic or cholinergic basal forebrain terminals evidenced by immunostaining for presynaptic vesicular transporter and postsynaptic scaffolding proteins. J Comp Neurol 499(4):645–661. https://doi.org/10.1002/cne.21131

Henny P, Jones BE (2006b) Vesicular glutamate (VGlut), GABA (VGAT), and acetylcholine (VACht) transporters in basal forebrain axon terminals innervating the lateral hypothalamus. J Comp Neurol 496(4):453–467. https://doi.org/10.1002/cne.20928

Herbert H, Moga MM, Saper CB (1990) Connections of the parabrachial nucleus with the nucleus of the solitary tract and the medullary reticular formation in the rat. J Comp Neurol 293(4):540–580

Herkenham M, Nauta WJ (1977) Afferent connections of the habenular nuclei in the rat. A horseradish peroxidase study, with a note on the fiber-of-passage problem. J Comp Neurol 173(1):123–146. https://doi.org/10.1002/cne.901730107

Higley MJ, Gittis AH, Oldenburg IA, Balthasar N, Seal RP, Edwards RH, Lowell BB, Kreitzer AC, Sabatini BL (2011) Cholinergic interneurons mediate fast VGluT3-dependent glutamatergic transmission in the striatum. PLoS One 6(4):e19155. https://doi.org/10.1371/journal.pone.0019155

Hikosaka O (2010) The habenula: from stress evasion to value-based decision-making. Nat Rev Neurosci 11(7):503–513. https://doi.org/10.1038/nrn2866

Hong S, Jhou TC, Smith M, Saleem KS, Hikosaka O (2011) Negative reward signals from the lateral habenula to dopamine neurons are mediated by rostromedial tegmental nucleus in primates. J Neurosci 31(32):11457–11471. https://doi.org/10.1523/JNEUROSCI.1384-11.2011

Hopkins DA, Holstege G (1978) Amygdaloid projections to the mesencephalon, pons and medulla oblongata in the cat. Exp Brain Res 32(4):529–547

Hur EE, Zaborszky L (2005) Vglut2 afferents to the medial prefrontal and primary somatosensory cortices: a combined retrograde tracing in situ hybridization study. J Comp Neurol 483(3):351–373. https://doi.org/10.1002/cne.20444

Irmak SO, de Lecea L (2014) Basal forebrain cholinergic modulation of sleep transitions. Sleep 37(12):1941–1951. https://doi.org/10.5665/sleep.4246

Jhou TC, Geisler S, Marinelli M, Degarmo BA, Zahm DS (2009a) The mesopontine rostromedial tegmental nucleus: a structure targeted by the lateral habenula that projects to the ventral tegmental area of Tsai and substantia nigra compacta. J Comp Neurol 513(6):566–596. https://doi.org/10.1002/cne.21891

Jhou TC, Fields HL, Baxter MG, Saper CB, Holland PC (2009b) The rostromedial tegmental nucleus (RMTg), a GABAergic afferent to midbrain dopamine neurons, encodes aversive stimuli and inhibits motor responses. Neuron 61(5):786–800. https://doi.org/10.1016/j.neuron.2009.02.001

Jones BE (2004) Activity, modulation and role of basal forebrain cholinergic neurons innervating the cerebral cortex. Prog Brain Res 145:157–169. https://doi.org/10.1016/S0079-6123(03)45011-5

Jourdain A, Semba K, Fibiger HC (1989) Basal forebrain and mesopontine tegmental projections to the reticular thalamic nucleus: an axonal collateralization and immunohistochemical study in the rat. Brain Res 505(1):55–65

Kaur S, Wang JL, Ferrari L, Thankachan S, Kroeger D, Venner A, Lazarus M, Wellman A, Arrigoni E, Fuller PM, Saper CB (2017) A genetically defined circuit for arousal from sleep during hypercapnia. Neuron. https://doi.org/10.1016/j.neuron.2017.10.009

Kirk IJ, McNaughton N (1991) Supramammillary cell firing and hippocampal rhythmical slow activity. Neuroreport 2(11):723–725

Kocsis B, Vertes RP (1994) Characterization of neurons of the supramammillary nucleus and mammillary body that discharge rhythmically with the hippocampal theta rhythm in the rat. J Neurosci 14(11 Pt 2):7040–7052

Kolmac C, Mitrofanis J (1999) Organization of the basal forebrain projection to the thalamus in rats. Neurosci Lett 272(3):151–154

Lee MG, Hassani OK, Jones BE (2005) Discharge of identified orexin/hypocretin neurons across the sleep-waking cycle. J Neurosci 25(28):6716–6720. https://doi.org/10.1523/JNEUROSCI.1887-05.2005

Lin SC, Nicolelis MA (2008) Neuronal ensemble bursting in the basal forebrain encodes salience irrespective of valence. Neuron 59(1):138–149. https://doi.org/10.1016/j.neuron.2008.04.031

Lin SC, Brown RE, Hussain Shuler MG, Petersen CC, Kepecs A (2015) Optogenetic dissection of the basal forebrain neuromodulatory control of cortical activation, plasticity, and cognition. J Neurosci 35(41):13896–13903. https://doi.org/10.1523/JNEUROSCI.2590-15.2015

Lu J, Sherman D, Devor M, Saper CB (2006) A putative flip-flop switch for control of REM sleep. Nature 441(7093):589–594. https://doi.org/10.1038/nature04767

Mahoney CE, Agostinelli LJ, Brooks JN, Lowell BB, Scammell TE (2017) GABAergic neurons of the central amygdala promote cataplexy. J Neurosci 37(15):3995–4006. https://doi.org/10.1523/JNEUROSCI.4065-15.2017

Martinez V, Parikh V, Sarter M (2005) Sensitized attentional performance and Fos-immunoreactive cholinergic neurons in the basal forebrain of amphetamine-pretreated rats. Biol Psychiatry 57(10):1138–1146. https://doi.org/10.1016/j.biopsych.2005.02.005

Matsumoto M, Hikosaka O (2007) Lateral habenula as a source of negative reward signals in dopamine neurons. Nature 447(7148):1111–1115. https://doi.org/10.1038/nature05860

Mayse JD, Nelson GM, Avila I, Gallagher M, Lin SC (2015) Basal forebrain neuronal inhibition enables rapid behavioral stopping. Nat Neurosci 18(10):1501–1508. https://doi.org/10.1038/nn.4110

McDonald AJ, Mascagni F (2010) Neuronal localization of m1 muscarinic receptor immunoreactivity in the rat basolateral amygdala. Brain Struct Funct 215(1):37–48. https://doi.org/10.1007/s00429-010-0272-y

Mileykovskiy BY, Kiyashchenko LI, Siegel JM (2005) Behavioral correlates of activity in identified hypocretin/orexin neurons. Neuron 46(5):787–798. https://doi.org/10.1016/j.neuron.2005.04.035

Miller RL, Knuepfer MM, Wang MH, Denny GO, Gray PA, Loewy AD (2012) Fos-activation of FoxP2 and Lmx1b neurons in the parabrachial nucleus evoked by hypotension and hypertension in conscious rats. Neuroscience 218:110–125. https://doi.org/10.1016/j.neuroscience.2012.05.049

Milner TA, Joh TH, Pickel VM (1986) Tyrosine hydroxylase in the rat parabrachial region: ultrastructural localization and extrinsic sources of immunoreactivity. J Neurosci 6(9):2585–2603

Moga MM, Herbert H, Hurley KM, Yasui Y, Gray TS, Saper CB (1990) Organization of cortical, basal forebrain, and hypothalamic afferents to the parabrachial nucleus in the rat. J Comp Neurol 295(4):624–661. https://doi.org/10.1002/cne.902950408

Nickerson Poulin A, Guerci A, El Mestikawy S, Semba K (2006) Vesicular glutamate transporter 3 immunoreactivity is present in cholinergic basal forebrain neurons projecting to the basolateral amygdala in rat. J Comp Neurol 498(5):690–711. https://doi.org/10.1002/cne.21081

Nunez A, Cervera-Ferri A, Olucha-Bordonau F, Ruiz-Torner A, Teruel V (2006) Nucleus incertus contribution to hippocampal theta rhythm generation. Eur J Neurosci 23(10):2731–2738. https://doi.org/10.1111/j.1460-9568.2006.04797.x

Olszewski J, Baxter DW (1953) Cytoarchitecture of the human brain stem. Anat Rec 115(2):435–435

Palmiter RD (2018) The parabrachial nucleus: CGRP neurons function as a general alarm. Trends Neurosci 41(5):280–293. https://doi.org/10.1016/j.tins.2018.03.007

Papez J (1937) A proposed mechanism of emotion. Arch Neurol Psychiatry 38:725–743

Pedersen NP, Ferrari L, Venner A, Wang JL, Abbott SBG, Vujovic N, Arrigoni E, Saper CB, Fuller PM (2017) Supramammillary glutamate neurons are a key node of the arousal system. Nat Commun 8(1):1405. https://doi.org/10.1038/s41467-017-01004-6

Petrovich GD, Swanson LW (1997) Projections from the lateral part of the central amygdalar nucleus to the postulated fear conditioning circuit. Brain Res 763(2):247–254

Pinto L, Goard MJ, Estandian D, Xu M, Kwan AC, Lee SH, Harrison TC, Feng G, Dan Y (2013) Fast modulation of visual perception by basal forebrain cholinergic neurons. Nat Neurosci 16(12):1857–1863. https://doi.org/10.1038/nn.3552

Price JL, Amaral DG (1981) An autoradiographic study of the projections of the central nucleus of the monkey amygdala. J Neurosci 1(11):1242–1259

Price JL, Stern R (1983) Individual cells in the nucleus basalis–diagonal band complex have restricted axonal projections to the cerebral cortex in the rat. Brain Res 269(2):352–356

Qin C, Luo M (2009) Neurochemical phenotypes of the afferent and efferent projections of the mouse medial habenula. Neuroscience 161(3):827–837. https://doi.org/10.1016/j.neuroscience.2009.03.085

Risold PY, Swanson LW (1997) Connections of the rat lateral septal complex. Brain Res Brain Res Rev 24(2–3):115–195

Rizvi TA, Ennis M, Behbehani MM, Shipley MT (1991) Connections between the central nucleus of the amygdala and the midbrain periaqueductal gray: topography and reciprocity. J Comp Neurol 303(1):121–131. https://doi.org/10.1002/cne.903030111

Rossi J, Balthasar N, Olson D, Scott M, Berglund E, Lee CE, Choi MJ, Lauzon D, Lowell BB, Elmquist JK (2011) Melanocortin-4 receptors expressed by cholinergic neurons regulate energy balance and glucose homeostasis. Cell Metab 13(2):195–204. https://doi.org/10.1016/j.cmet.2011.01.010

Rye DB, Wainer BH, Mesulam MM, Mufson EJ, Saper CB (1984) Cortical projections arising from the basal forebrain: a study of cholinergic and noncholinergic components employing combined retrograde tracing and immunohistochemical localization of choline acetyltransferase. Neuroscience 13(3):627–643

Rye DB, Saper CB, Lee HJ, Wainer BH (1987) Pedunculopontine tegmental nucleus of the rat: cytoarchitecture, cytochemistry, and some extrapyramidal connections of the mesopontine tegmentum. J Comp Neurol 259(4):483–528. https://doi.org/10.1002/cne.902590403

Saper CB (1984) Organization of cerebral cortical afferent systems in the rat. II. Magnocellular basal nucleus. J Comp Neurol 222(3):313–342. https://doi.org/10.1002/cne.902220302

Saper CB (2016) The house alarm. Cell Metab 23(5):754–755. https://doi.org/10.1016/j.cmet.2016.04.021

Scammell T, Gerashchenko D, Urade Y, Onoe H, Saper C, Hayaishi O (1998) Activation of ventrolateral preoptic neurons by the somnogen prostaglandin D2. Proc Natl Acad Sci USA 95(13):7754–7759

Schwaber JS, Rogers WT, Satoh K, Fibiger HC (1987) Distribution and organization of cholinergic neurons in the rat forebrain demonstrated by computer-aided data acquisition and three-dimensional reconstruction. J Comp Neurol 263(3):309–325. https://doi.org/10.1002/cne.902630302

Semba K (2000) Multiple output pathways of the basal forebrain: organization, chemical heterogeneity, and roles in vigilance. Behav Brain Res 115(2):117–141

Shammah-Lagnado SJ, Alheid GF, Heimer L (2001) Striatal and central extended amygdala parts of the interstitial nucleus of the posterior limb of the anterior commissure: evidence from tract-tracing techniques in the rat. J Comp Neurol 439(1):104–126. https://doi.org/10.1002/cne.1999

Shi YF, Han Y, Su YT, Yang JH, Yu YQ (2015) Silencing of cholinergic basal forebrain neurons using archaerhodopsin prolongs slow-wave sleep in mice. PLoS One 10(7):e0130130. https://doi.org/10.1371/journal.pone.0130130

Shibata H (1989) Descending projections to the mammillary nuclei in the rat, as studied by retrograde and anterograde transport of wheat germ agglutinin-horseradish peroxidase. J Comp Neurol 285(4):436–452. https://doi.org/10.1002/cne.902850403

Swanson LW, Cowan WM (1979) The connections of the septal region in the rat. J Comp Neurol 186(4):621–655. https://doi.org/10.1002/cne.901860408

Swanson LW, Mogenson GJ, Gerfen CR, Robinson P (1984) Evidence for a projection from the lateral preoptic area and substantia innominata to the 'mesencephalic locomotor region' in the rat. Brain Res 295(1):161–178

Tokita K, Inoue T, Boughter JD Jr (2009) Afferent connections of the parabrachial nucleus in C57BL/6J mice. Neuroscience 161(2):475–488. https://doi.org/10.1016/j.neuroscience.2009.03.046

Tovote P, Esposito MS, Botta P, Chaudun F, Fadok JP, Markovic M, Wolff SB, Ramakrishnan C, Fenno L, Deisseroth K, Herry C, Arber S, Luthi A (2016) Midbrain circuits for defensive behaviour. Nature 534(7606):206–212. https://doi.org/10.1038/nature17996

Unal CT, Pare D, Zaborszky L (2015) Impact of basal forebrain cholinergic inputs on basolateral amygdala neurons. J Neurosci 35(2):853–863. https://doi.org/10.1523/JNEUROSCI.2706-14.2015

Veening JG, Swanson LW, Sawchenko PE (1984) The organization of projections from the central nucleus of the amygdala to brainstem sites involved in central autonomic regulation: a combined retrograde transport-immunohistochemical study. Brain Res 303(2):337–357

Vertes RP (2015) Major diencephalic inputs to the hippocampus: supramammillary nucleus and nucleus reuniens. Circuitry and function. Prog Brain Res 219:121–144. https://doi.org/10.1016/bs.pbr.2015.03.008

Vong L, Ye C, Yang Z, Choi B, Chua S Jr, Lowell BB (2011) Leptin action on GABAergic neurons prevents obesity and reduces inhibitory tone to POMC neurons. Neuron 71(1):142–154. https://doi.org/10.1016/j.neuron.2011.05.028

Voytko ML, Olton DS, Richardson RT, Gorman LK, Tobin JR, Price DL (1994) Basal forebrain lesions in monkeys disrupt attention but not learning and memory. J Neurosci 14(1):167–186

Wallace DM, Magnuson DJ, Gray TS (1992) Organization of amygdaloid projections to brainstem dopaminergic, noradrenergic, and adrenergic cell groups in the rat. Brain Res Bull 28(3):447–454

Wilkinson LS, Dias R, Thomas KL, Augood SJ, Everitt BJ, Robbins TW, Roberts AC (1997) Contrasting effects of excitotoxic lesions of the prefrontal cortex on the behavioural response to D-amphetamine and presynaptic and postsynaptic measures of striatal dopamine function in monkeys. Neuroscience 80(3):717–730

Woolf NJ, Butcher LL (1982) Cholinergic projections to the basolateral amygdala: a combined Evans Blue and acetylcholinesterase analysis. Brain Res Bull 8(6):751–763

Wyss JM, Swanson LW, Cowan WM (1979) Evidence for an input to the molecular layer and the stratum granulosum of the dentate gyrus from the supramammillary region of the hypothalamus. Anat Embryol (Berl) 156(2):165–176

Xu M, Chung S, Zhang S, Zhong P, Ma C, Chang WC, Weissbourd B, Sakai N, Luo L, Nishino S, Dan Y (2015) Basal forebrain circuit for sleep-wake control. Nat Neurosci 18(11):1641–1647. https://doi.org/10.1038/nn.4143

Yetnikoff L, Lavezzi HN, Reichard RA, Zahm DS (2014) An update on the connections of the ventral mesencephalic dopaminergic complex. Neuroscience 282:23–48. https://doi.org/10.1016/j.neuroscience.2014.04.010

Yokota S, Kaur S, VanderHorst VG, Saper CB, Chamberlin NL (2015) Respiratory-related outputs of glutamatergic, hypercapnia-responsive parabrachial neurons in mice. J Comp Neurol 523(6):907–920. https://doi.org/10.1002/cne.23720

Yoshida K, McCormack S, Espana RA, Crocker A, Scammell TE (2006) Afferents to the orexin neurons of the rat brain. J Comp Neurol 494(5):845–861. https://doi.org/10.1002/cne.20859

Zaborszky L, Duque A (2003) Sleep-wake mechanisms and basal forebrain circuitry. Front Biosci 8:d1146–1169

Zahm DS, Cheng AY, Lee TJ, Ghobadi CW, Schwartz ZM, Geisler S, Parsely KP, Gruber C, Veh RW (2011) Inputs to the midbrain dopaminergic complex in the rat, with emphasis on extended amygdala-recipient sectors. J Comp Neurol 519(16):3159–3188. https://doi.org/10.1002/cne.22670